

**Catalytic application of carbon nanotubes obtained from plastic  
solid waste in the removal of quinoline from isooctane by selective  
oxidation with hydrogen peroxide**

**Larissa De Grande Piccinin**

Thesis report submitted to  
**Escola Superior de Tecnologia e Gestão**  
**Instituto Politécnico de Bragança**  
Master Degree in  
**Chemical Engineering**

Supervisors:

**Prof. Helder Teixeira Gomes**

**Prof. Admilson Lopes Vieira**

**Dr. Jose Luis Díaz de Tuesta**

Bragança  
2022

**Catalytic application of carbon nanotubes obtained from plastic solid waste in the removal of quinoline from isooctane by selective oxidation with hydrogen peroxide**

**Larissa De Grande Piccinin**

Thesis report submitted to **Escola Superior de Tecnologia e Gestão** of **Instituto Politécnico de Bragança** to obtain the Master Degree in Chemical Engineering in the ambit of the double diploma with the **Universidade Tecnológica Federal do Paraná - Câmpus Londrina**

Supervisors:

**Prof. Helder Teixeira Gomes**

**Prof. Admilson Lopes Vieira**

**Dr. Jose Luis Díaz de Tuesta**

Bragança

2022



## ACKNOWLEDGEMENTS

First, I want to thank God for guiding my path to this achievement, for the opportunity to live this life experience. To my parents, Helena and Osmair for encouraging me to face all the difficulties of this last year, for always supporting me and for the comfort of being always present in my life!

To my supervisors Dr. Helder T. Gomes of Instituto Politécnico de Bragança (IPB) and professor Dr. Admilson Lopes Vieira of Universidade Tecnológica Federal do Paraná (UTFPR) for entrusting me with the work and for giving me all the necessary support by the development of this.

I thank the research group in which I was inserted, which became my friends, as well as co-workers, and whom I admire so much. To Dr. Jose Luis Díaz de Tuesta for all his patience, teachings and advice during this time of work. To Msc. Adriano Silva for all the help and for relaxing any environment. Especially, Msc. Fernanda Roman who taught me so much inside the laboratory, helped me every day, who entrusted me with the task of carrying out research related to her work and who developed me a lot as a person and professional. Finally, Msc. Ana Paula Silva, my roommate who became a sister, who helped me since before I arrived in Portugal, who supported me so much and held my hand every day for the last year. I was so lucky!

To my family for supporting me to continue the journey even physically distant, to my uncles Benedita and Odair for supporting me. To my friends from Santa Adélia - SP and Bragança, Portugal.

I thank the Universidade Tecnológica Federal do Paraná – Câmpus Londrina for the opportunity to carry out the double degree in another country, the Polytechnic Institute of Bragança for the reception and for offering the structure and professionals in the development of this work. To CIMO for the opportunity and knowledge acquired.

This work is a result of project PLASTIC\_TO\_FUEL&MAT (POCI 01 0145-FEDER-031439) and CIMO (UIDB/00690/2020) financed through FCT/MCTES (PIDDAC).



## ABSTRACT

Different carbon nanotubes were tested in two-phase oxidative processes using hydrogen peroxide as oxidant in order to remove and degrade a model contaminant, quinoline, from isooctane, which simulated contaminated fossil fuels. The CNTs were produced by chemical vapor deposition (CVD) from different polymers. The use of low density polyethylene (LDPE), high density polyethylene (HDPE), polypropylene (PP) and a mixture of these three in the proportion of 35:25:40, respectively, resulted in the CNTs defined as CNT LDPE 600, CNT LDPE 800, CNT HDPE 800, CNT PP 800 and CNT MIX 800, where 600 or 800 represent the temperature of pyrolysis considered in the synthesis. The use of such polymers simulated the production of CNTs from residual plastic.

Prior to the biphasic oxidation runs, the organic phase underwent oxidation tests, being concluded that isooctane was not oxidized under the conditions used. Possible adsorption on the materials was also tested in the organic phase and in the biphasic medium. In both cases no significant adsorption was obtained. The produced CNTs were tested as catalysts in the oxidative processes of hydrogen peroxide in aqueous solution (CWPO) and in the biphasic medium. The performance of each material was analyzed in 24-hour reaction tests, at 80 °C, through monitorization of H<sub>2</sub>O<sub>2</sub> degradation, quinoline concentration in oily and aqueous media, total organic carbon concentration, aromatics concentration in oily and aqueous media, and pH measurement.

In addition to the tests carried out with the CNTs produced, a commercial CNT was also tested for comparison. Finally, all catalysts used fulfilled the proposed objective, 100% of quinoline being removed from the oily phase in the biphasic oxidation runs, up to 8 h of reaction, and degrading 100% of the contaminant by CWPO in 4 h. Other analyses revealed a complete degradation of H<sub>2</sub>O<sub>2</sub> with all CNTs in the CWPO tests and in the biphasic oxidation runs, except for the commercial CNT in the biphasic oxidation run. The analysis of TOC and aromatics concentration show significant decreases with all tested carbon nanomaterials, while pH had a slight decrease in the CWPO runs and an increase in the biphasic oxidation runs. In summary, all carbon materials produced were efficient in the proposed process and are comparable to the performance obtained by the commercial CNT.

**Keywords:** oxidative denitrification, quinoline, biphasic oxidation, carbon nanomaterials, hydrogen peroxide.

## RESUMO

Diferentes nanotubos de carbono foram testados em processos oxidativos bifásicos usando peróxido de hidrogênio como oxidante para remover e degradar um contaminante modelo, quinolina, do isooctano, o qual simulou combustíveis fósseis no processo. Os CNTs foram produzidos por deposição química em fase vapor (CVD) a partir de diferentes polímeros: polietileno de baixa densidade (LDPE), polietileno de alta densidade (HDPE), polipropileno (PP) e uma mistura destes três na proporção de 35:25:40, respectivamente. Os quais foram identificados como: CNT LDPE 600, CNT LDPE 800, CNT HDPE 800, CNT PP 800 e CNT MIX 800, onde 600 ou 800 representam a temperatura de pirólise considerada na síntese. O uso de tais polímeros simulou a produção de CNTs a partir de plástico residual.

Antes das corridas de oxidação bifásica, a fase orgânica foi submetida a testes de oxidação, concluindo-se que o isooctano não foi oxidado nas condições utilizadas. A possível adsorção nos materiais também foi testada na fase orgânica e no meio bifásico. Em ambos os casos não foi obtida adsorção significativa. Os CNTs produzidos foram testados como catalisadores nos processos oxidativos do peróxido de hidrogênio em solução aquosa (CWPO) e no meio bifásico. O desempenho de cada material foi analisado em reações de 24 horas, a 80 °C, através do monitoramento da degradação de H<sub>2</sub>O<sub>2</sub>, concentração de quinolina em meio oleoso e aquoso, concentração de carbono orgânico total, concentração de aromáticos em meio oleoso e aquoso e medição de pH.

Além dos testes realizados com os CNTs produzidos, também foi testado um CNT comercial para comparação. Por fim, todos os catalisadores utilizados atenderam ao objetivo proposto, sendo 100% da quinolina removida da fase oleosa nas corridas de oxidação bifásica, até 8 h de reação, e degradando 100% do contaminante por CWPO em 4 h. Outras análises revelaram uma degradação completa do H<sub>2</sub>O<sub>2</sub> com todos os CNTs nos testes de CWPO e nas corridas de oxidação bifásica, exceto para o CNT comercial na corrida de oxidação bifásica. A análise da concentração de TOC e aromáticos mostrou decréscimos significativos com todos os nanomateriais de carbono testados, enquanto o pH teve uma ligeira diminuição nas execuções de CWPO e um aumento nas execuções de oxidação bifásica. Em resumo, todos os materiais de carbono produzidos foram eficientes no processo proposto e são comparáveis ao desempenho obtido pelo CNT comercial.

**Palavras-chave:** desnitrificação oxidativa, quinolina, oxidação bifásica, nanomateriais de carbono, peróxido de hidrogênio.

## TABLE OF CONTENTS

LIST OF FIGURES .....	vi
LIST OF TABLES .....	viii
LIST OF ACRONYMS .....	ix
1 INTRODUCTION .....	1
1.1 MOTIVATION .....	1
1.2 OBJECTIVES .....	3
1.3 REPORT OUTLINE .....	3
2 STATE OF THE ART .....	4
2.1 FOSSIL FUELS .....	4
2.1.1 ISOCTANE .....	5
2.1.2 CONTAMINANT COMPOUNDS IN FUELS .....	6
2.1.3 NITROGEN-CONTAINING COMPOUNDS FROM FUELS .....	7
2.2 REMOVAL OF NITROGENATED AND SULFONATED COMPOUNDS FROM FUELS .....	8
2.3 OXIDATIVE DENITROGENATION .....	9
2.3.1 QUINOLINE .....	11
2.3.2 HYDROGEN PEROXIDE .....	13
2.3.3 BIPHASIC SYSTEMS .....	16
2.3.4 CATALYSTS IN ODN PROCESSES .....	18
2.3.4.1 CARBON CATALYST .....	19
2.3.4.2 PROCESSES FOR PRODUCTION OF CNTs .....	20
2.4 PLASTIC SOLID WASTE .....	21
3 MATERIALS AND METHODS .....	23
3.1 REACTANTS AND EQUIPMENTS .....	23
3.2 SYNTHESIS OF CNTs .....	25
3.3 PRELIMINARY TESTS WITH THE OILY PHASE .....	26
3.3.1 TRANSFER OF ISOCTANE TO WATER .....	26
3.3.2 ISOCTANE OXIDATION .....	27
3.3.3 MASS TRANSFER OF QUINOLINE FROM OIL TO WATER .....	27
3.4 ANALYTICAL METHODS .....	28
3.4.1 UV/VIS .....	28
3.4.2 HPLC .....	28
3.4.3 pH ANALYSIS .....	28
3.4.4 TOTAL ORGANIC CARBON ANALYSIS .....	28
3.4.5 FT-IR .....	29
3.5 ADSORPTION OF QUINOLINE .....	29
3.5.1 IN OILY PHASE .....	29
3.5.2 IN A BIPHASIC MEDIUM .....	29
3.6 OXIDATION OF QUINOLINE .....	29
3.6.1 OXIDATION IN AQUEOUS PHASE .....	30

3.6.2	BIPHASIC OXIDATION .....	31
4	RESULTS AND DISCUSSION .....	32
4.1	PRELIMINARY TESTS ON OILY PHASE.....	32
4.1.1	TRANSFER OF ISOCTANE TO WATER .....	32
4.1.2	ISOCTANE OXIDATION.....	32
4.1.3	MASS TRANSFER OF QUINOLINE.....	34
4.2	DEVELOPMENT OF ANALYTICAL TECHNIQUES.....	35
4.2.1	DETERMINATION OF H <sub>2</sub> O <sub>2</sub> CONCENTRATION.....	35
4.2.2	DETERMINATION OF QUINOLINE CONCENTRATION BY SPECTROPHOTOMETRY ....	38
4.2.2.1	DETERMINATION OF QUINOLINE IN OILY PHASE.....	38
4.2.2.2	DETERMINATION OF QUINOLINE IN AQUEOUS PHASE .....	40
4.2.3	DETERMINATION OF QUINOLINE CONCENTRATION BY HPLC .....	43
4.2.4	DETERMINATION OF AROMATICS .....	44
4.3	ADSORPTION OF QUINOLINE.....	46
4.3.1	ORGANIC ADSORPTION .....	46
4.3.2	BIPHASIC ADSORPTION .....	47
4.4	CATALYTIC WET PEROXIDE OXIDATION (CWPO) .....	49
4.4.1	CONCENTRATION OF HYDROGEN PEROXIDE IN CWPO RUNS.....	49
4.4.2	CONCENTRATION OF QUINOLINE IN CWPO RUNS.....	50
4.4.3	TOTAL ORGANIC CARBON IN CWPO .....	52
4.4.4	ANALYSIS OF AROMATICS IN CWPO.....	54
4.4.5	ANALYSIS OF pH IN CWPO .....	54
4.5	BIPHASIC OXIDATION .....	55
4.5.1	CONCENTRATION OF HYDROGEN PEROXIDE IN AQUEOUS PHASE .....	55
4.5.2	CONCENTRATION OF QUINOLINE IN OILY PHASE.....	57
4.5.3	QUINOLINE CONCENTRATION IN AQUEOUS PHASE .....	59
4.5.4	TOTAL ORGANIC CARBON IN AQUEOUS PHASE .....	61
4.5.5	AROMATIC ANALYSIS IN OILY PHASE.....	62
4.5.6	AROMATIC ANALYSIS IN AQUEOUS PHASE .....	63
4.5.7	pH ANALYSIS IN AQUEOUS PHASE .....	63
5	CONCLUSION AND FUTURE WORK.....	65
5.1	CONCLUSION .....	65
5.2	FUTURE WORK .....	65
	REFERENCES.....	67
	ATTACHMENTS .....	72

## LIST OF FIGURES

Figure 1. Examples of pyridinic and pyrrolic compounds drawn in ChemSketch Software [25].	7
Figure 2. Papers published on HDN, ODS and ODN over the years until December/2021 (source: SCOPUS with the keywords “hydrodenitrogenation”, “oxidative desulfurization” and “oxidative denitrogenation”).	10
Figure 3. Chemical properties of quinoline extracted from software ACD/3D Viewer.	12
Figure 4. Figure collected from the study of researchers S. Ravi and S. Vadukumpully (2016) exemplifying the main formats of graphene as a 2D building block that can assume different dimensionalities: 0D fullerenes, 1D nanotubes or 3D graphite [70].	21
Figure 5. Percentages of the main plastics consumed in European Union and some applications of each one of them, image extracted from “The Facts – Plastics Europe 2020”, a study developed by the Plastic Europe-Association of Plastics Manufactures [15].	22
Figure 6. Typical look of CNTs synthesized from polymers.	26
Figure 7. Setup for oxidation experiments.	30
Figure 8. Final product of biphasic oxidations.	31
Figure 9. Isooctane oxidation test during 24 h (80 °C, pH 3, W/O = 20/80, $C_{H_2O_2} = 247$ g/L).	33
Figure 10. FT-IR spectra of pure isooctane in comparison with isooctane samples after oxidation reactions: a) complete and b) fingerprint spectra.	33
Figure 11. Mass transfer of quinoline into the aqueous phase from oily phase (W/O = 20/80) at different concentrations: (a) 250, (b) 500, (c) 750 and (d) 1000 mg/L (80 °C, pH 3 in aqueous phase).	35
Figure 12. Calibration curve for the determination of $H_2O_2$ concentration in the CWPO experiments carried out with 100 mg/L of quinoline in aqueous solution.	37
Figure 13. Calibration curve for determination of $H_2O_2$ concentration in the experiments carried out with quinoline concentration of 1000 mg/L.	37
Figure 14. Calibration curve for the determination of quinoline concentration in isooctane solutions.	38
Figure 15 - Spectra of quinoline in ethanol.	39
Figure 16. Calibration curve for the determination of quinoline concentration in isooctane solutions diluted with ethanol.	40
Figure 17. Spectra from different concentration of (a) quinoline aqueous solution and (b) $H_2O_2$ .	41
Figure 18. Calibration curve of quinoline in aqueous medium by UV/VIS.	42
Figure 19. $H_2O_2$ concentration in the wavelength of 313 nm.	43
Figure 20. Calibration curve for the determination of quinoline concentration in aqueous solutions by HPLC.	44
Figure 21. Calibration curve for the determination of aromatics in oily medium as quinoline.	45
Figure 22. Calibration curve for the determination of aromatic compounds in aqueous medium based on the concentration of quinoline.	46
Figure 23. Adsorption of quinoline on the CNTs over contact time (80 °C, $C_{CNT} = 2,5$ g/L, $C_{QN} = 1000$ mg/L in isooctane).	47
Figure 24. Adsorption of quinoline under a biphasic system (80 °C, W/O = 20/80, $C_{CNT} = 2.5$ g/L, $C_{QN,0} = 1000$ mg/L in isooctane).	48
Figure 25. Example of biphasic system in the biphasic adsorption runs.	48
Figure 26. Hydrogen peroxide concentration measured by UV/VIS in CWPO runs (80 °C, pH <sub>0</sub> 3, $C_{QN} = 100$ mg/L in water, $C_{CNT} = 2.5$ g/L, $C_{H_2O_2} = 6.2$ g/L).	50
Figure 27. Concentration of quinoline in CWPO runs (80 °C, pH <sub>0</sub> 3, $C_{QN} = 100$ mg/L in water, $C_{CNT} = 2.5$ g/L, $C_{H_2O_2} = 6.2$ g/L).	51
Figure 28. Reaction intermediates identified by the different retention times in HPLC (80 °C, pH <sub>0</sub> 3, $C_{QN} = 100$ mg/L in water, $C_{H_2O_2} = 6.2$ g/L).	52
Figure 29. Percentages of TOC removal from oxidation in an aqueous system (80 °C, pH <sub>0</sub> 3, $C_{QN} = 100$ mg/L in water, $C_{CNT} = 2.5$ g/L, $C_{H_2O_2} = 6.2$ g/L).	53
Figure 30. Aromatic removal after 24 h of run (80 °C, pH <sub>0</sub> 3, $C_{QN} = 100$ mg/L in water, $C_{CNT} = 2.5$ g/L, $C_{H_2O_2} = 6.2$ g/L).	54
Figure 31. Analysis of pH after 24 h of CWPO run (80 °C, pH <sub>0</sub> 3, $C_{QN} = 100$ mg/L in water, $C_{CNT} = 2.5$ g/L, $C_{H_2O_2} = 6.2$ g/L).	55
Figure 32. Concentration of hydrogen peroxide in the biphasic oxidation runs (80 °C, pH <sub>0</sub> 3 in aqueous phase, $C_{QN} = 1000$ mg/L in isooctane, $C_{CNT} = 2.5$ g/L, $C_{H_2O_2} = 247$ g/L).	56
Figure 33. Concentration of quinoline in the oily phase in biphasic oxidation runs (80 °C, pH <sub>0</sub> 3 in aqueous phase, $C_{QN} = 1000$ mg/L in isooctane, $C_{CNT} = 2.5$ g/L, $C_{H_2O_2} = 247$ g/L).	58

Figure 34. Biphasic system after 24 h of oxidation reaction. ....	59
Figure 35. Quinoline quantity by UV-VIS in aqueous phase in biphasic oxidation runs (80 °C, pH <sub>0</sub> 3 in aqueous phase, C <sub>QN</sub> = 1000 mg/L in isooctane, C <sub>CNT</sub> = 2.5 g/L, C <sub>H<sub>2</sub>O<sub>2</sub></sub> = 247 g/L). ....	60
Figure 36. Final spectra of aqueous phase after the biphasic oxidation. ....	61
Figure 37. TOC results from aqueous phase after 24 h of biphasic oxidation runs (80 °C, pH <sub>0</sub> 3 in aqueous phase, C <sub>QN</sub> = 1000 mg/L in isooctane, C <sub>CNT</sub> = 2.5 g/L, C <sub>H<sub>2</sub>O<sub>2</sub></sub> = 247 g/L). ....	62
Figure 38. Aromatic removal in oily phase after 24 h of biphasic oxidation runs (80 °C, pH <sub>0</sub> 3 in aqueous phase, C <sub>QN</sub> = 1000 mg/L in isooctane, C <sub>CNT</sub> = 2.5 g/L, C <sub>H<sub>2</sub>O<sub>2</sub></sub> = 247 g/L). ....	62
Figure 39. Aromatic removal in aqueous phase after 24 h of biphasic oxidation runs (80 °C, pH <sub>0</sub> 3 in aqueous phase, C <sub>QN</sub> = 1000 mg/L in isooctane, C <sub>CNT</sub> = 2.5 g/L, C <sub>H<sub>2</sub>O<sub>2</sub></sub> = 247 g/L). ....	63
Figure 40. Analysis of pH after 24 h of biphasic oxidation runs (80 °C, pH <sub>0</sub> 3 in aqueous phase, C <sub>QN</sub> = 1000 mg/L in isooctane, C <sub>CNT</sub> = 2.5 g/L, C <sub>H<sub>2</sub>O<sub>2</sub></sub> = 247 g/L). ....	64

## LIST OF TABLES

Table 1. Examples of experimental conditions of ODN processes using H <sub>2</sub> O <sub>2</sub> as oxidant. ....	15
Table 2. Operating conditions of studies reporting oxidation of quinoline with hydrogen peroxide in biphasic and emulsified systems.....	17

## LIST OF ACRONYMS

1Me-IND	1-methyl-substituted indole
2Me-IND	2-methyl-substituted indole
3Me-IND	3-methyl-substituted indole
4,6-DMDBT	4,6 di-methyl dibenzothiophene
ADS	Adsorptive desulfurization
AND	Adsorptive denitrogenation
AOP	Advanced oxidation process
BDN	Biodenitrogenation
BDS	Biodesulfurization
BT	Benzothiophene
$C_{CNT}$	Carbon nanotubes concentration
CCVD	Catalytic chemical vapor deposition
$C_{H_2O_2}$	Hydrogen peroxide concentration
CNF	Carbon nanofibers
CNT	Carbon nanotubes
CODN	Catalytic oxidative denitrogenation
CODS	Catalytic oxidative desulfurization
$C_{oil}$	Quinoline concentration in isooctane (mol/kg)
$C_{QN}$	Quinoline concentration
CRZ	Carbazole
CVD	Chemical vapor deposition
CWAO	Catalytic wet air oxidation
$C_{water}$	Quinoline concentration in water (mol/kg)
CWPO	Catalytic wet peroxide oxidation
DBT	Dibenzothiophene
ECODS	Extractive and catalytic oxidative desulfurization
EDN	Extractive denitrogenation
EDS	Extractive desulfurization
FCC	Fluid catalytic cracking
Gli 400	Limonite-glycerol treated at 400°C
HDM	Hydrodemetalation
HDN	Hydrodenitrogenation
HDO	Hydrodeoxygenation
HDS	Hydrodesulfurization

IND	Indole
K	Partition coefficient
LPG	Liquefied petroleum gas
MANC	Magnetic amphiphilic nanocomposites
Mtoe	Million tons of oil equivalent
NCC	Nitrogen-containing organic compound
N.C	Non-catalytic
ODN	Oxidative denitrogenation
ODS	Oxidative desulfurization
ONC	Organonitrogen compounds
PAH	Polycyclic aromatic hydrocarbon
PCDN	Photocatalytic denitrogenation
PCDS	Photocatalytic desulfurization
PNA	Polynuclear aromatics
ppmw	Parts per million by weight
PRL	Pyrrole
QN	Quinoline
SCC	Sulfur-containing organic compound
UAOD	Ultrasound assisted oxidative desulfurization and denitrogenation
VGO	Vacuum gas oil
W <sub>2</sub> N(x)@C	Tungsten nitride-incorporated carbon
wt %	Weight %

## 1 INTRODUCTION

### 1.1 MOTIVATION

The global energy demand has experienced a steady growth due to the global upsurge in population and industrialization. Between 1971 and 2017, world energy consumption has increased by almost three times, reaching a value around 13,972 Mtoe in 2017. Among the several types of energy resources, fossil fuels represent the primary source of energy all over the world [1]. The COVID-19 crisis caused a historic decline in global oil demand in 2020, but not necessarily a lasting effect, and the global oil demand is expected to increase for years to come [2].

Development or even existence at the present level of standard of living requires energy to move on [3]. However, there are economic and environmental issues associated with fossil fuels due to the increasing energy demand [1]. Therefore, even more, new technologies must be developed to soften the damages suffered by the environment.

In the area of crude oil treatment, oil-refining industries need to cope with the specifications of commercialized fuels, which are driven by environmental concerns. Sulfur and nitrogen levels are among those main concerns. In this sense, refineries or end users' terminals need to convert fuel oil into higher quality products [4]. Sulfur and nitrogen-containing compounds are converted into gases such as  $\text{SO}_x$  and  $\text{NO}_x$  during combustion. Thus, their content in fuels should be limited to control these emissions. Those gases are known as acidic gases owing to their contribution towards acid rain, being able to blend with water and other particles before reaching the ground [5].

Among the  $\text{NO}_x$  group ( $\text{NO}$ ,  $\text{NO}_2$  and  $\text{N}_2\text{O}$ ),  $\text{NO}_2$  deserves special attention since it is converted to nitric acid with compounds present in the atmosphere and reduces visibility, besides the harmful effects to human beings, including chronic bronchitis, dyspnea and pulmonary edema [5]. Thus, an increase in rigidity in the emissions of  $\text{NO}_x$  has been observed worldwide.

The conventional treatment of crude oils consists of separation, conversion, and treatment processes. Among the separation processes, distillation is the most used and aims at separating compounds by their boiling points. Fluid catalytic cracking is a typical example of a conversion aimed at reducing the length of carbon chains compared to the initial feed [6]. Treatment processes, as hydrotreating, aims at cleaning fuels by removing contaminants, such as sulfur and nitrogen compounds [7].

Nowadays, hydrotreating is the main process used to achieve low levels of nitrogen in fuels, being also referred to as hydrodenitrogenation (HDN). However, this process requires extremely high operational conditions of pressure and temperature, being thus considered limited. A complementary or alternative process is the oxidative denitrogenation (ODN) [8]. This technique targets the oxidation of nitrogen-containing compounds to form oxygenated derivatives [9].

ODN needs an oxidant to generate hydroxyl radicals (HO<sup>•</sup>), the main responsible for the oxidation of the target organic compounds in the process. Dealing with the current concerns about the environment, hydrogen peroxide is considered a green oxidant commonly used for this purpose. Hydrogen peroxide presents high efficiency as oxidant and it is not an expensive product [10]. However, hydrogen peroxide is lipophobic, a mechanism interconnecting the target contaminant with the oxidant being required to degrade the nitrogen compounds present in the fuel [11]. A biphasic system is in this case formed by an aqueous phase, in which H<sub>2</sub>O<sub>2</sub> is solubilized, and the oily phase (fuel). In the oxidation process, a catalyst has to be present to initiate the decomposition of hydrogen peroxide and to help the mass transfer between the two phases [12]. There are several materials presenting suitable catalytic activity, and carbon-based materials have received increased attention due to the low-cost and ecofriendly character of the methods used to produce them from several carbon sources.

Carbon nanotubes (CNTs) have been largely used as catalysts in many processes due to their interesting characteristics [13]. Their attractiveness increases when they are obtained from carbon-containing wastes, under a perspective of circular economy. In this sense, plastic solid waste (PSW) can be used as carbon source. PSW is generated from several areas, such as medical equipment, packaging, construction, electronics, electrical goods, furniture, automobiles, households and agriculture [14]. In 2019, the global plastic production was around 368 million tons, with European share corresponding to 57.9 million tons. Currently, Europe is responsible for 16% of the global plastic production distributed in several sectors [15]. Thus, PSW needs a better destination, and their transformation into a valorized product is an attractive idea.

## 1.2 OBJECTIVES

The objective of this work is to study the applications of PSW derived CNTs aiming at the denitrification of a simulated fuel by ODN. Oxidation will be carried out with hydrogen peroxide as oxidant in a biphasic system containing water and an oily phase (isooctane). Quinoline was chosen as model nitrogenated compound. The CNTs have been prepared from PSW at different conditions, in a previous research work carried out in the group where this thesis has been developed. It is expected to address the following issues for the success of this work:

1. Study the adsorption of quinoline using the prepared CNTs at different conditions, both in organic and biphasic medium;
2. Evaluate the decomposition of hydrogen peroxide with the selected CNTs while in the presence of quinoline;
3. Evaluate the ability of the CNTs towards the abatement of quinoline in an aqueous medium;
4. Assess the catalytic activity of the CNTs in the removal of quinoline in a biphasic system.

## 1.3 REPORT OUTLINE

This MSc thesis is divided in 5 chapters, including the present one, where the motivation to study the removal of N and S-containing compounds in fuels, the main objectives to be fulfilled and the proposed organization to present and discuss the developed studies are presented.

The second chapter addresses general aspects of fossil fuels, treatments for the denitrification of fuel oils, the ODN process with hydrogen peroxide in a biphasic system, the CNTs used as catalysts in ODN, and the production process of CNTs from plastic waste.

In chapter 3, the chemicals and materials, as well as the equipment and experimental methodology employed in this study, are described. In chapter 4, the experimental results are presented and discussed. Finally, in chapter 5, the main conclusions of this thesis are summarized. Additionally, some suggestions for future work are indicated in order to improve and complete the studies developed and presented in this thesis.

## 2 STATE OF THE ART

### 2.1 FOSSIL FUELS

The demand for energy increases constantly, fossil fuels being the most common sources to supply that need. However, fossil fuels are a non-renewable energy source [16]. Main transportation fuels are products derived from crude oil found in deep reserves. The composition of crude oils includes countless sorts of hydrocarbons with different physical and chemical properties. Generally, the composition consists of carbon (83–87 wt %), hydrogen (10–14 wt %), sulfur (< 6.0 wt %), nitrogen (< 2.0 wt %) and oxygen (< 1.5 wt %). By physical and chemical treatments occurring at petroleum refineries, crude oil is transformed in transportation fuels and chemicals [17].

Economically, the process of converting crude oil into commercial products depends on the crack spread, which is defined as the difference between the price of a barrel of crude oil and the cumulative price of all petroleum final products that are refined from that crude oil, and the value is an approximation of a refinery's margin, and the wider is the spread, the more profitable is the refinery [18].

Petroleum refineries have been generally developed for the production of transportation fuels, such as gasoline, diesel and kerosene, with the production of building blocks for the petrochemicals, such as light alkenes (ethylene, propylene, butene and butadiene) and BTEX (benzene, toluene, ethylbenzene and xylene) [17].

The refinery industry can be considered a multiproduct manufacturing plant, which aims at transforming crude oil into end-user products. The refining process is divided into three basic steps: separation, conversion and treatment [6].

The first step, separation, consists in atmospheric and vacuum distillation, in which the compounds are separated based on their boiling points [17]. The residual oil from the vacuum distillation is known as vacuum gas oil (VGO) which consists in the heavy fraction of the crude oil. In the second step, conversion, VGO is transformed into gasoline and other hydrocarbons. In the petrochemical refinery, the main conversion process is the fluid catalytic cracking process (FCC) [7]. The conversion processes have been focused mainly on reducing long chain hydrocarbons [6].

FCC process consists of two main reaction zones. The first is when a hot particulate catalyst is contacted with the VGO feedstock, producing cracked products (final products with a smaller carbon chain than the initial feed). The second is the coked

catalyst. After the first reaction, the stream of cracked products and the catalyst are separated and the coked catalyst is burned in a regenerator at 650–760 °C and 2 bar, aiming the regeneration of the catalyst, which represent the second reaction zone of FCC. During a FCC process, several reactions take place, such as cracking, hydrogen transfer, isomerization and coking [7].

Another process similar to FCC is hydrocracking, in which the goal is the production of gasoline and light oil for diesel fuel and kerosene for domestic fuel from VGO. This process has been originated for the production of gasoline after the Second World War. A bifunctional catalyst is included in the process for cracking and hydrogenation/dehydrogenation with high pressurized hydrogen, around approximately 250 °C, a temperature lower than used in FCC [17]. Once crude oil has been subjected to separation and conversion, the resultant products are ready for purification, which consists mainly on the removal of contaminants [6]. This last process is known as treatment.

Nowadays, around 85% of fuels derive from crude oil. Crude oil is a mixture of different hydrocarbons, such as aliphatic, cyclic and aromatic compounds, and organic components containing heteroatoms, such as sulfur, nitrogen and oxygen. The composition of crude oil depends on its geographical origin [19]. The presence of nitrogen and sulfur-containing compounds in crude oil implies that the crude oil goes through pretreatment steps and even specialized processes in the refineries [9]. These compounds affect the environment and humans due to emissions of oxides, such as NO<sub>x</sub> and SO<sub>x</sub>, during the combustion of fuels. Those oxides are associated with acid rains, affecting the ozone layer, and serious health threats for human beings, including respiratory diseases, such as asthma, bronchitis, emphysema and throat inflammation [20].

Despite the damaging consequences from fossil fuels combustion, they are energetically viable, whenever methods to reduce the concentration of contaminants can be developed [9].

### 2.1.1 ISOOCTANE

In scientific research aiming to analyze a treatment process applied on fuels, a model compound can simulate its behavior. In this work, isooctane or 2,2,4-trimethylpentane, was chosen as a representative of gasoline fraction.

Isooctane is a single hydrocarbon that represent gasoline because of some of its important properties. It is an octane isomer (C<sub>8</sub>H<sub>18</sub>) with a molecular weight of 114.23 g/mol and a boiling point of 98–99 °C. This compound is an important substance in gasoline because it is used in a relatively large proportion to upturn the fuel's knock resistance [21].

The boiling point of pure isooctane is very different from that of gasoline. Gasoline is a multi-substance (C<sub>4</sub>–C<sub>12</sub>) with a multi boiling point between 27 and 225 °C [21]. In addition, isooctane is a major component in spark ignition engine fuels. It is widely used as a model or surrogate compound in reactions to simulate the behavior of fuels [22].

Another important parameter is the solubility of isooctane in water. A study [23] affirms that with the increase of temperature, the solubility of isooctane in water also increases. At 298 K, the mole fraction solubility of isooctane is  $(0.44 \pm 0.05) \times 10^{-6}$ . At 323 K, it increases to  $(0.52 \pm 0.04) \times 10^{-6}$  and at 373 K the mole fraction solubility is  $(2.0 \pm 0.1) \times 10^{-6}$ . Lastly, increasing the temperature to 473 K increases the mole fraction solubility to  $(61 \pm 1) \times 10^{-6}$ . All those measures obtained at 65 bar of pressure [23].

## 2.1.2 CONTAMINANT COMPOUNDS IN FUELS

Contaminant compounds in crude oil and in their products are present as organosulfur, nitrogen-, and oxygen- compounds, known as heteroatoms [24]. The use of fossil fuels in both stationary (heating and thermal power plants, petroleum refineries) and mobile (automotive engines) combustion sources, results in the transformation of those compounds into oxide species, such as SO<sub>2</sub>, NO and NO<sub>2</sub>. These species are considered the most toxic and harmful gases emitted into the atmosphere. Flue gas streams from fossil-fuel-fired power plants are responsible for 87% of SO<sub>x</sub> and 67% of NO<sub>x</sub> emissions [25].

As a consequence of the contaminants produced by the combustion of fossil fuels, industrialized countries have stringent legal threshold values for the content of sulfur in transportation fuels, below 10 ppmw S for gasoline and diesel in the European Union [24]. But, despite the fact that nitrogen oxides from the use of fossil fuels also damage the environment, there is no limiting specifications about nitrogen-containing compounds in fuels [25].

The existing specifications that control nitrogen-containing compounds have the target of maintaining NO<sub>x</sub> emissions below the regulatory levels of 30 mg/km (defined by Euro VI). Nitrogen levels are also controlled by indirect analysis, such as gum content, storage stability and thermal stability of the fuel [25].

### 2.1.3 NITROGEN-CONTAINING COMPOUNDS IN FUELS

Some of the nitrogen-containing compounds found in fuel oils are quinoline, indoles, carbazoles, benzcarbazoles, pyridines, pyrrole, azapyridines, aniline, phenantridines and porphyrins, among others [24].

In about 90% of crude oils, the content of nitrogen is lower than 0.25 wt %, which has become a reference. Accordingly, if the oil is composed by more than 0.25 wt % of N, the nitrogen concentration is considered high. If the levels are below 0.25 wt % of N, the oil is considered poor in nitrogen-containing compounds. Nitrogen compounds in crude oils are conventionally divided in two groups: the basic, which are derivatives of pyridine, and non-basic nitrogen compounds, coming from pyrrole. Some examples of nitrogenated compounds can be seen in Figure 1 [25].

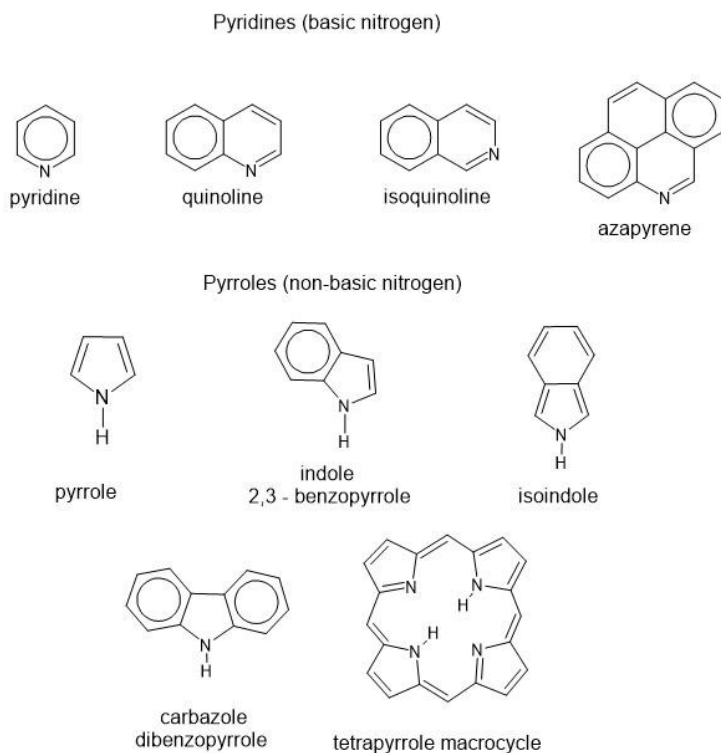


Figure 1. Examples of pyridinic and pyrrolic compounds drawn in ChemSketch Software [25].

## 2.2 REMOVAL OF NITROGENATED AND SULFONATED COMPOUNDS FROM FUELS

Treatment is the final process of refining, which includes combining processed products to create various octane levels, vapor pressure properties and targeted properties for products used in extreme environments. Another goal of the treatment step is the removal of contaminant compounds, such as sulfur and nitrogen [6].

The importance of removing sulfur and nitrogen has two reasons. The first are the desired levels of these two elements in the final fuel, and the second is the need to avoid poisoning the catalyst. Basic nitrogen-containing compounds deactivate the solid acidic catalysts. One way to avoid it is to remove them by adsorptive denitrogenation, by stirring the oil with the solid in a batch reactor at room temperature. However, it is difficult to regenerate the adsorbent at a low temperature after chemisorption, and thus the adsorbates need to be eliminated from the adsorbent by combustion [17].

The goal of achieving low levels of sulfur and nitrogen compounds can be accomplished by processes such as hydrodesulfurization (HDS) and hydrodenitrogenation (HDN), oxidative desulfurization (ODS) and denitrogenation (ODN), extractive desulfurization (EDS) and denitrogenation (EDN), adsorptive desulfurization (ADS) and denitrogenation (AND), photocatalytic desulfurization (PCDS) and denitrogenation (PCDN), biodesulfurization (BDS) and denitrogenation (BDN), ultrasound assisted oxidative desulfurization and denitrogenation (UAOD) [26].

The two most common specific treatments for commercial fuels and applied on an industrial scale in the refineries are hydrotreating (HDS and HDN). HDS and HDN are responsible for the removal of sulfur and nitrogen compounds, respectively, from polyaromatic compounds from heavy gas oil feedstocks. These two techniques require  $H_2$  and a catalyst. The typical catalyst includes Co-Mo and Ni-Mo sulfides, and the typical conditions employed are temperatures in the range of 300-450 °C and pressure of 35-170 bar [7].

HDS and HDN occur simultaneously. Similarly, the operating conditions used also enable the removal of metals (known as hydrodemetalation, HDM) and of oxygen (known as hydrodeoxygenation, HDO) [7]. During HDS and HDN,  $H_2S$  and  $NH_3$ , respectively, are formed. These two gaseous compounds can be easily removed from the product stream by distillation. This process is very efficient for the removal of thiols,

sulfides and disulfides. But the removal of heterocyclic sulfur compounds to the required values is hard to attain [19]. Aliphatic nitrogen is readily removed during HDN, but the removal of aromatic nitrogen requires ring saturation before denitrogenation [27].

Thus, to further lower the sulfur and nitrogen contents to achieve the established threshold values, severe hydrotreating operating conditions are required, such as higher pressures, temperatures, and hydrogen flow rates. Increasing the temperature leads to oil cracking and higher pressures lead to an increase in the saturation of aromatics and higher hydrogen consumption. Thus, the consequences of those operating conditions are the decline in catalyst lifespan and the degradation of oil quality, besides requiring a huge capital investment for high-pressure processes [8].

Alternatively, non-hydrogenation approaches for effective ultra-deep desulfurization and denitrogenation have attracted research interests, such as ODN and ODS. They are simple processes with low cost techniques, operating at mild conditions (25-130 °C and 1-5 atm). Hydrogen peroxide (H<sub>2</sub>O<sub>2</sub>) is frequently considered as a oxidant source in ODN and ODS processes due to its strong oxidizing ability and low cost [28].

In this work, the focus is on the removal of nitrogen-containing compounds by oxidative denitrogenation, ODN, which is less expanded than ODS, even though they occur at the same time when both compounds are present in the stream.

### 2.3 OXIDATIVE DENITROGENATION

The oldest study regarding ODN found in Scopus database is from the author Jack Lewis, in the year 1979 [29] (keyword search: oxidative denitrogenation, date of search: 24/03/2022). From the first study in 1979 to the year 2000, only five specific research studies in this area are found. Currently, in the Scopus platform, 58 studies for ODN can be found, which is a very low amount compared to ODS, where 2,405 publications are reported (keyword search: oxidative desulfurization, date of search: 24/03/1997) for the period 1951-2021. Figure 2 displays the number of publications in ODN, HDN and ODS.

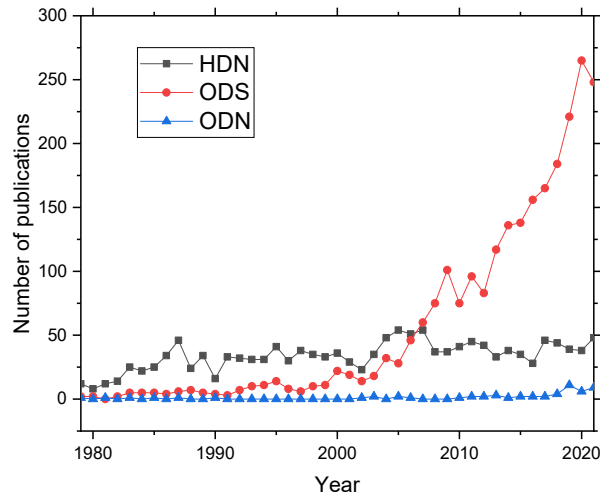


Figure 2. Papers published on HDN, ODS and ODN over the years until December/2021 (source: SCOPUS with the keywords “hydrodenitrogenation”, “oxidative desulfurization” and “oxidative denitrogenation”).

ODN targets the oxidation of nitrogen-containing compounds to form oxygenated derivatives. This is complementary to catalytic hydrodenitrogenation (hydrotreating), or HDN, a well-known technique employed by the refining industries to eliminate nitrogen by formation of ammonia as product [9].

Nitrogen compounds present in crude oil are predominantly heterocyclic aromatic compounds and the remaining are aliphatic compounds, such as amines and nitriles. Heterocyclic nitrogen compounds are harder to remove by hydrotreating, as mentioned in section 2.2. Thus, oxidative denitrogenation can be seen as a complementary technique to hydrotreating [30].

The operating conditions of ODN are moderate, including atmospheric pressure, temperature lower than 100 °C, and an oxidant compound, such as H<sub>2</sub>O<sub>2</sub>, O<sub>2</sub> or O<sub>3</sub>. After the oxidation, the resultant oxidized nitrogen compounds are significantly more polar than the nitrogen compounds of the initial stream and can be extracted by a polar solvent to remove those compounds from oil [31]. As a result, the extraction with appropriate non-miscible solvent or adsorbent can guarantee the fuel quality to the desired level [26]. Most commonly used solvents include dimethyl sulfoxide (DMSO), dimethylformamide (DMF), acetonitrile, methanol and acetone. Some disadvantages of solvent extraction are toxicity, reusability, disposal, explosiveness and cost. An alternative solvent is water to soften the extraction consequences. The proper selection of solvent is a challenge [8].

Due to the extraction, aiming to separate the oxidized nitrogen compounds, the removal of nitrogen from oil is accompanied by a loss of fuel, since the principle is to remove the nitrogen-containing compounds instead of only nitrogen. As an example of this point, the loss of hydrocarbon material for an oil containing 1 wt % of nitrogen may be in the order of 10–20 wt % of the oil. This is due to the molecules with a high amount of carbon and hydrogen comparing to the number of nitrogen atoms in the organic nitrogen compounds found in the oils [27].

Comparing the ODN and ODS processes, the oxidation of nitrogen-containing organic compounds (NCCs) is considered a complex oxidation because of its chemical properties. The N atom on NCCs and the S atom on sulfur-containing organic compounds (SCCs) are second-row and third-row elements, respectively. Thus, a smaller N can accommodate only one oxygen atom and, on the other hand, a larger S can have a maximum of two oxygen atoms, during the oxidation process. Besides the fact that NCCs can be harder to oxidize, there are fewer specific studies about ODN [32].

Most of the studies dealing with ODN explore the removal of N using quinoline as a model pollutant [19, 30-32]. In the present work, quinoline will also be considered as model component.

### 2.3.1 QUINOLINE

Quinoline and its derivatives are the primary nitrogenous organic contaminant present in crude oils [36]. It is part of a group called PNA-compounds (polynuclear aromatics), closely related to polycyclic aromatic hydrocarbons (PAHs) [37]. The molecules of quinoline are representative of nitrogen-heterocyclic compounds, with a nitrogen-atom incorporated in the ring system, as shown in Figures 1 and 3 [38].

Quinoline is often used as raw material and solvent in the manufacture of paints, dyes, herbicides, and other fine chemicals. It can be originated from coal tar, mineral oil and petroleum, and from industrial wastewaters, such as coking, coal gasification and pharmaceutical wastewaters [39].

The molecule quinoline is slowly transformed biologically into some less toxic compounds, such as 2-hydroxyquinoline [37]. Owing to this slow degradation, low biodegradability and high solubility in aqueous solutions, quinoline is considered a common contaminant of groundwaters and soils [38]. The solubility of quinoline in water

depends strongly on the pH of the aqueous phase. At a pH of 4.5, acidified with HCl, the solubility of quinoline is 61.31 mg/mL. Otherwise, in a system containing only water, at a pH of 6.31, the solubility of quinoline is 0.05 mg/mL [40].

Another point that deserves attention is the characteristic toxicity, carcinogenicity, and mutagenicity of quinoline. These characteristics are dangerous to the environment, inhibiting microorganisms' growth, threatening plants, animals, and human beings. Quinoline is considered as a priority organic pollutant by the US Environmental Protection Agency [39].

Accordingly, aiming to avoid the presence of toxic compounds in the environment, like quinoline, there are many studies about techniques to reduce the contaminant levels on fuels, such as HDN, HDS, ODN and ODS [9].

The oxidation of quinoline is a complex reaction. In the literature, it is reported that the carbon with the least electron density in the ring of an organonitrogen compound is oxidized by peroxides and then ring opening follows. The ring opening causes the formation of various possible oxygenated products of ketone and carboxylic acid category [8]. Figure 3 shows with more detail the molecule of quinoline and some of its chemical properties.

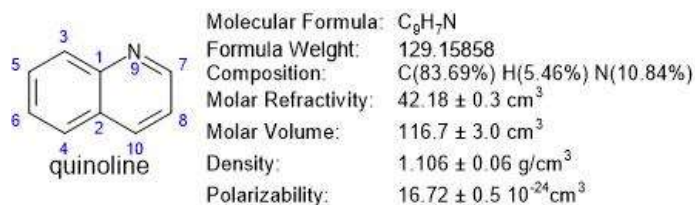


Figure 3. Chemical properties of quinoline extracted from software ACD/3D Viewer.

Some of the reported identified intermediates obtained by ozonation of quinoline in aqueous phase are 2-hydroxyquinoline, 8-hydroxyquinoline, o-amino benzaldehyde, salicylic acid, quinolinic acid, formamide, N-phenyl-, formic acid, acetic acid and oxalic acid [39].

Other reported intermediate compounds from catalytic wet air oxidation (CWAO) of quinoline in aqueous phase includes acetic acid, nicotinic acid, succinic acid and oxalic acid, which are further slowly oxidized to CO<sub>2</sub>, water, NO<sub>x</sub> and N<sub>2</sub> [38]. Another example

of a final product of oxidation of quinoline is quinoline-N-oxide, a compound identified after an oxidation process using hydrogen peroxide as oxidant [24].

In addition, the oxidation of nitrogen compounds increases their polarity, which makes it easy to remove organonitrogen compounds from oily phases by adsorption or extraction, thus resulting in oxidative denitrogenation (ODN) [8].

### 2.3.2 HYDROGEN PEROXIDE

Hydrogen peroxide ( $\text{H}_2\text{O}_2$ ) is a compound used as oxidant, discovered by Thénard as early as 1818. Its commercial production was mastered around 1930s in many European countries, Soviet Union, Korea, Japan, United States and Australia [41].  $\text{H}_2\text{O}_2$  is a colorless, odorless, and slightly acidic liquid. It is considered an atom-efficient, benign and eco-friendly oxidant. Depending on the application of hydrogen peroxide, it can have concentrations ranging between 30 and 70% [42].

Oxidation reactions play an important role in organic processes, and the search for more selective and efficient oxidants is a current need, since society has placed restrictions on industrial oxidation technology, with an emphasis on the need for sustainability [10]. Greener processes can be attained by following three main directives: (i) minimization of the number of by-products and waste, (ii) use of benign reactants and solvents, and (iii) use of selective catalysts [43].

$\text{H}_2\text{O}_2$  is an adequate oxidant, showing a high efficiency per weight of oxidant. Hydrogen peroxide and molecular oxygen (air can often be used) are examples of environmentally friendly oxidants since they do not give rise to any waste product. Due to this characteristic, there is an increasing demand to use them [10].

Comparing molecular oxygen with hydrogen peroxide, the use of oxygen in oxidation processes has the disadvantage that rigorous safety handling is required for large-scale applications but, on the other hand, it is inexpensive (air). While with hydrogen peroxide, the industrial chemists appreciate its miscibility with water and relatively easiness of handling, it can undergo radical-induced decomposition to  $\text{H}_2\text{O}$  and  $\text{O}_2$  with impurities in the system [10].

Another important and attractive characteristic of oxidation with hydrogen peroxide is the moderate conditions that can be considered, such as temperatures between

25 and 130°C and pressures of 1 to 5 atm, if reactions are carried out in the presence of a suitable catalyst [44].

The process mechanism is based on solubilized hydrogen peroxide molecules in water and, with the presence of an appropriate catalyst, hydrogen peroxide is dissociated, producing hydroxyl radicals (HO•), which is the main responsible for oxidizing the organic compounds in the medium [45]. Reactions between HO• and organic compounds undergo with the abstraction of H atoms from C–H, N–H or O–H bonds, and hydroxyl radical's addition to unsaturated bonds like C=C bonds or aromatic rings [46].

The mechanism can be represented by equations (1) to (7), as a general example of the oxidation reaction. “R” is the organic compound containing nitrogen that will be oxidized [37].

Initiation:



Propagation:



Termination:



The reaction can be divided into three parts: initiation, propagation, and termination. The first part is when the catalyst works as the initiator to decompose hydrogen peroxide, the second part is when the active substances react among them, and the third part is when the intermediates are produced [37].

An example of a known Advanced Oxidation Process (AOP) that uses hydrogen peroxide as oxidant is Catalytic Wet Peroxide Oxidation (CWPO) [45]. Nowadays, due to its high efficiency proved during studies and researches, AOPs have been widely used and known as “clean technologies”, with the possibility of becoming the most used wastewater treatment processes in the future [47].

The mechanisms involved in AOPs include the generation of extremely reactive HO• radicals, responsible for the oxidation of pollutants in the wastewaters [48]. The role

of those radicals is to attack, quickly and non-selectively, all oxidizable substances [49]. The main difference between the goal of CWPO to treat wastewater and its application in the present work is the need for selectivity. The selective oxidation with hydrogen peroxide intends to achieve only the oxidation of the pollutant, quinoline in this case, but not the oxidation of the fuel.

Considering the optimized conditions in the AOP, the result will be closer to the complete degradation of the organic contaminant compounds present in water and further treatment will be exempt [45]. These organic pollutants are oxidized to harmless products or CO<sub>2</sub> when mineralization happens [50]. In addition, a liquid discharge will not be necessary, because the contaminants were mineralized, or partially mineralized, and the water became clean, without the need for a separation process, such as extraction, adsorption or others [49].

Another difference between ODN and CWPO is related to the fact that ODN occurs in a biphasic system (oil-water), with the oxidant present in the aqueous phase and the pollutant present in the oily phase. So, it is necessary to discharge the water with the oxidized compounds.

Table 1. Examples of experimental conditions of ODN processes using H<sub>2</sub>O<sub>2</sub> as oxidant.

Ref.	Contaminant	Organic phase	Molar ratio (O/N)	Catalyst	Reaction time (min)	Temperature (°C)	Final conversion (%)
[33]	Organo-nitrogen compounds (ONCs) (1000 ppm)	n-octane	N/M	W <sub>2</sub> N(x)@C	120	37	60
[51]	Pyridine (800 ppm)	Fuel oil	16	Acid-functionalized [Bmim]Cl/ZnCl <sub>2</sub> (Ionic liquid)	60	45	100
[34]	BT (646 ppmw), DBT (1493.8 ppmw), 4,6-DMDBT (646 ppmw), and QN (445 ppmw) BT (2650 ppmw), DBT (6150 ppmw), 4,6-DMDBT (2650 ppmw), and QN (1335 ppmw)	2, 2, 4-trimethyl pentane (20 v.% toluene)	4	Vanadium substituted Dawson-type phosphotungstate	60	70	95 (BT, DBT, 4,6-DMDBT) 100 (QN) 87 (BT, DBT, 4,6-DMDBT) 100 (QN)

There are some specific experimental conditions which are very important to analyze the ODN process, such as the organic phase as fuel model, the mole ratio of oxidizer to nitrogen (O/N), the catalyst, reaction time, temperature, and the kind of

contaminant. In this work quinoline will be used, but there are some published studies working with more than one contaminant in the same solution [33, 34]. Table 1 shows some examples of these studies.

### 2.3.3 BIPHASIC SYSTEMS

Biphasic systems are composed of at least two immiscible liquids, such as water and oils. Besides the phases, there is the interphase zone which is the boundary between the immiscible liquids [52]. Those processes are useful for a range of products/reactions, such as Suzuki coupling, aldol condensation, olefin hydroformylation, vegetable oil hydrolysis, biomass conversion, polymerization and oxidation [11]. In an oxidation process, a system with two phases limits the mass transfer through the biphasic interphases, leading to a decrease in the oxidation rate. Most of the reported oxidative systems, such as ODS and ODN, involve the use of oil-insoluble oxidants, such as  $H_2O_2$ , or other peroxides, which results in a biphasic oil-aqueous solution system [53].

Hydrogen peroxide, a low cost and commercially available promising oxidizing agent, water soluble, as mentioned before, can be used for the selective oxidation of different substrates, such as olefins, hydrocarbons and other organic molecules [11]. Due to the oxidants used in ODN, soluble in polar solvents, such as water, ODN requires a biphasic system, with the fuels with sulfur and nitrogen contaminants being present in the non-polar oily phase. Therefore, the oxidation of the contaminants is low due to the limited interface between these two phases (oil/water), making the oxidation process very difficult [54].

In this situation, the oxidation of the lipophilic organic pollutants (present in the oil phase) may be controlled by the mass transfer of the pollutants from the oil phase to the aqueous phase and by the properties of the pollutant partition coefficient between these phases of that specific system. Thereby, high hydrophilic pollutants will be preferably present in the aqueous phase (low partition coefficient and more concentrated in the aqueous phase), allowing their contact with hydrogen peroxide and making easy the oxidation reaction [44]. Generally, the contaminants from fuels are preferably in the oily phase.

For this reason, the presence of an efficient catalyst in the oxidation is very important because this is the system's main condition to promote the oxidation reaction

and the mass transfer between the phases. Hybrid materials are very interesting for biphasic reactions, as they have an amphiphilic character, meaning that they can interact simultaneously with aqueous and oily phases, increasing the interface between the phases [54].

Amphiphilic materials introduced into a two-phase system will be preferably located at the oil/water interface. If stirred, the materials will be preferably located on the surface of the dispersed droplets of one phase into the other, thereby forming an emulsion. In an emulsion, the interface between the two phases is enhanced by promoting greater contact between them [54]. Those composites are used as emulsifiers or demulsifiers in different processes, such as petroleum, vegetable oils, biodiesel and wastewater treatment [11].

In addition, solid particles promoting phase transfer processes can be more easily recovered. Recently, composites based on hydrophobic carbon nanomaterials supported on hydrophilic oxide particles have been used to stabilize water-oil emulsions and catalyze reactions at the liquid-liquid interface [55]. Due to the development of those applications, highly efficient robust amphiphilic nanostructures have been identified as an important challenge for further research, as for example carbon nanotubes (CNTs) [55].

Table 2. Operating conditions of studies reporting oxidation of quinoline with hydrogen peroxide in biphasic and emulsified systems.

Ref.	QN concentration	Organic phase	W/O ratio	O/N ratio (mol/mol)	Catalyst	Removal of QN
[11]	N/M	Cyclohexane	N/M	N/M	MANCs	100
[11]	N/M	Cyclohexane	N/M	N/M	-	10
[53]	50	Toluene	1/99	N/M	Gli 400	97
[54]	50	Cyclohexane	17/83	4,5	Fe/C and FeMo/C	100
[55]	500	Cyclohexane	24/76	0,01	CNTs	100
[55]	500	Cyclohexane	24/76	0,01	-	10
[56]	30	Cyclohexane	17/83	7,6	N-doped CNTs	80
[56]	30	Cyclohexane	17/83	7,6	pure CNTs	44
[57]	500	Cyclohexane	17/83	0,45	red mud	100
[57]	500	Cyclohexane	17/83	0,45	-	10
[58]	N/M	Cyclohexane	N/M	N/M	Copper (II)	100
[58]	N/M	Cyclohexane	N/M	N/M	-	10

Table 2 summarizes some of the experimental conditions applied in oxidative processes with hydrogen peroxide in biphasic systems aiming to oxidize quinoline similar to those considered in the present work.

Most of the studies considered emulsified systems, differently from the objective of this project. In this work, we aim at testing different catalysts produced by our research team under biphasic systems, without the formation of emulsions. Although emulsions systems can provide an interesting platform for biphasic reactions due to increased interfacial area, it also requires extra-effort into producing the emulsions to carry out the reactions. Breaking the emulsion and recovering the phase of interest could also prove more demanding when working under emulsified systems.

#### 2.3.4 CATALYSTS IN ODN PROCESSES

ODN with the application of a catalyst can also be known as catalytic oxidative denitrogenation (CODN), a process that is considered as potentially efficient and viable for the removal of nitrogen-containing compounds from fuel oils [51].

The catalyst must accomplish some behaviors, such as stabilizing the microstructure or active components, formation of new compounds to act as active components or stabilizers, having two or more functions. Also, influencing the rate of adsorption/desorption and diffusion of molecules and the migration or transference of the active species [59].

In ODN processes using hydrogen peroxide, the catalyst is responsible for initiating the decomposition of hydrogen peroxide. It can also participate as an adsorbent and it can affect the mass transfer between the two phases. Due to the catalytic activity,  $H_2O_2$  could be activated into active substances under low-temperature conditions [12].

Another important characteristic for catalysts in biphasic systems is displaying amphiphilicity. An amphiphilic material presents the potential of simultaneous interaction with a polar and a non-polar compound. It means that an amphiphilic catalyst would be interacting with the aqueous and the oily phases at the same time, increasing mass transfer, allowing the stabilization of biphasic systems and catalyzing reactions at the liquid/liquid interface in oxidative processes [60].

Carbon catalysts are emerging green catalytic materials that recently attracted much attention due to its environmental friendliness and high efficiency. Nanocarbon

materials can be examples because they have demonstrated superior catalytic performance than traditional metal catalysts in many fields, such as hydrocarbon conversion, fine chemicals production, fuel cells, solar energy [61], and oxidation reactions for the removal of contaminants in wastewater treatments [62, 63]. Carbon-based catalysts have thus become a promising research topic in the area. Furthermore, several studies have applied carbon-based materials for ODN purposes, as displayed in Tables 1 and 2.

#### 2.3.4.1 CARBON CATALYST

Since the second half of the 20<sup>th</sup> century, carbon-based nanostructured materials have been studied as catalytic support materials in various chemical areas. Some advantages of carbon-based materials have been highlighted in heterogeneous catalytic reactions, amongst which are included chemical steadiness in both acid or basic medium, low corrosion capability, strong thermal constancy, hydrophobic behavior, retrieval from the reaction mixture and low price. A lot of carbon-based nanostructures have been discovered in the last three decades, including fullerenes, carbon nanotubes (CNTs), graphene, mesoporous carbons, carbon nanofibers (CNFs), among others [13]. Some examples of those structures are presented in Figure 4.

Discovered by Iijima (Japan) in 1991 [64], CNTs are allotropes of carbon. They consist in tubes with one or multiple layers (walls) of graphene sheets, leading to single and multi-walled CNTs (SWCNTs and MWCNTs, respectively). Their length is in the order of micrometers and the diameter in the order of nanometers [65].

CNTs can be used in several applications, including as catalysts or catalyst supports in the fields of renewable energy (storage and generation) and environmental technologies, such as oxidation, remediation or adsorption [66]. The tensile strength of CNTs is 100 times higher than stainless steels ( $\approx 150$  GPa) and its density about one-sixth ( $1100\text{-}1300$  kg/m<sup>3</sup>). Their thermal conductivity is comparable to that of diamonds ( $3000$  W/m/K) and their electric conductivity comparable to copper [67].

Also, the properties of CNTs, such as high surface area, sorption capacity and selectivity, make them potential sorbents for organic solutes in aqueous solutions [48]. CNTs are also stable in both acidic and alkaline media, with the advantage of reducing, or even eliminating, diffusion limitations, due to their relatively high surface area and absence of microporosity [66].

#### 2.3.4.2 PROCESSES FOR PRODUCTION OF CNTs

Currently, the existing methods of production require a lot of energy and resources. Some examples are the electric arc discharge method, laser ablation method, catalytic chemical vapor deposition (CVD), flame synthesis and the solar energy route [67].

When the goal is large-scale production of CNTs (10,000 tons of CNTs per year), the most promising and preferred method is Catalytic Chemical Vapor Deposition (CCVD) [67]. The CCVD method is considered a simple and low-cost method [56], involving a carbon-rich precursor that will interact with a catalyst at high temperature (600 – 1200 °C), to result in carbon deposition and in the growth of CNTs or CNFs at the catalyst surface. The carbon-rich precursor can be either a gas, a liquid or a solid, opening up possibilities for the upcycling of waste materials, such as PSW [68]. If PSW is used as carbon precursor, the PSW initially undergoes pyrolysis, producing volatile hydrocarbons that will be used as feedstock in CCVD [69].

During pyrolysis, the carbon-rich precursor is cracked in a furnace under an inert carrier gas to generate gaseous carbon-containing components. The cracking products interact with the catalyst on which the growth of the carbon nanotube takes place [70]. The resulting CNT depends on a series of operational conditions, such as temperature, steam, feedstock, feed rate, reactor type and catalyst [69].

The type of catalyst applied to facilitate the obtention of CNTs is very important to the process. Currently, the most common transition metals used as a catalyst are Fe, Ni and Co. Ni has a high ability to break C–C and C–H bonds, while Fe is more cost-effective. But bimetallic catalysts, such as Ni-Fe, Ni-Cu and Fe-Mo have been shown to be more efficient towards CNTs production. In addition, the bimetallic catalysts show a better activity and selectivity than single-metal catalysts during the reaction to produce CNTs, and can minimize the agglomeration of nano-sized active metal particles [69].

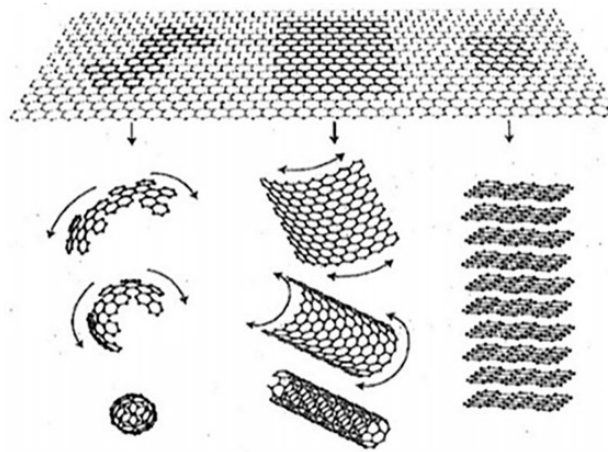


Figure 4. Figure collected from the study of researchers S. Ravi and S. Vadukumpully (2016) exemplifying the main formats of graphene as a 2D building block that can assume different dimensionalities: 0D fullerenes, 1D nanotubes or 3D graphite [70].

## 2.4 PLASTIC SOLID WASTE

Plastic materials, or polymers, are common in most products from many different sectors and are present in large quantities around the world. The word ‘plastic’ came from the Greek word ‘plastikos’ and means to be molded in different shapes [14]. The reason why plastic is so frequently found in people routines is because of its characteristics that can fit the plastics into a big mix of the production process. Some of these characteristics or properties are lightweight, low cost, durability, robustness, strength, corrosion resistance, thermal and electrical insulation, versatile fabrication and design capabilities [71].

The main consequence of that high consumption is the amount of waste at the end of the plastic chain. Nowadays, the waste plastics present in the environment is the major issue and several strategies are being adopted to fix it, which includes recycling, deposition in landfill, incineration, microbial degradation and conversion into useful materials [72]. Being non-degradable, these plastic wastes undergo photo-degradation, which turns them into plastic dust that affects the food cycle of living and this reason increases the importance of solid plastic waste management [73].

The polymers’ chemical structure represents a group of organic molecules with a high quantity of carbon atoms composed of small monomer molecules connected by a linking group with a covalent bond. The final products can have a lot of different properties, depending on their synthesis conditions [74]. The monomers can be compared

with bricks of a big building called polymer. Generally, they are simple molecules with a double bond or with a minimum of two active functional groups, one of those being responsible by the addition of one monomer molecule upon the other repeatedly, generating the final polymer by the polymerization reaction [75].

Polymer applications are widely used all around the world, such as packaging, building and construction, corrosion prevention and control, automotive, aerospace, electrical and electronic, agriculture and horticulture, domestic appliances, business machines, medical, biomedical, marine, offshore and sports [76].

Between all those areas and types of polymers, there are three of them representing almost 50% of all the plastics demand distribution, published by the Plastics Europe 2020 (4) (Figure 5). They are polypropylene (PP), low-density polyethylene (LDPE) and high-density polyethylene (HDPE) [15].

Thus, several novel methodologies are being developed to apply the waste plastics in some useful products, such as in the synthesis of carbon nanomaterials as CNTs. The use of plastic polymers as the carbonaceous feed and the transformation of the waste plastics into highly value-added products, such as CNTs, and working on a feasible process, will help solve the waste plastic issue and CNT production shortcomings [67].

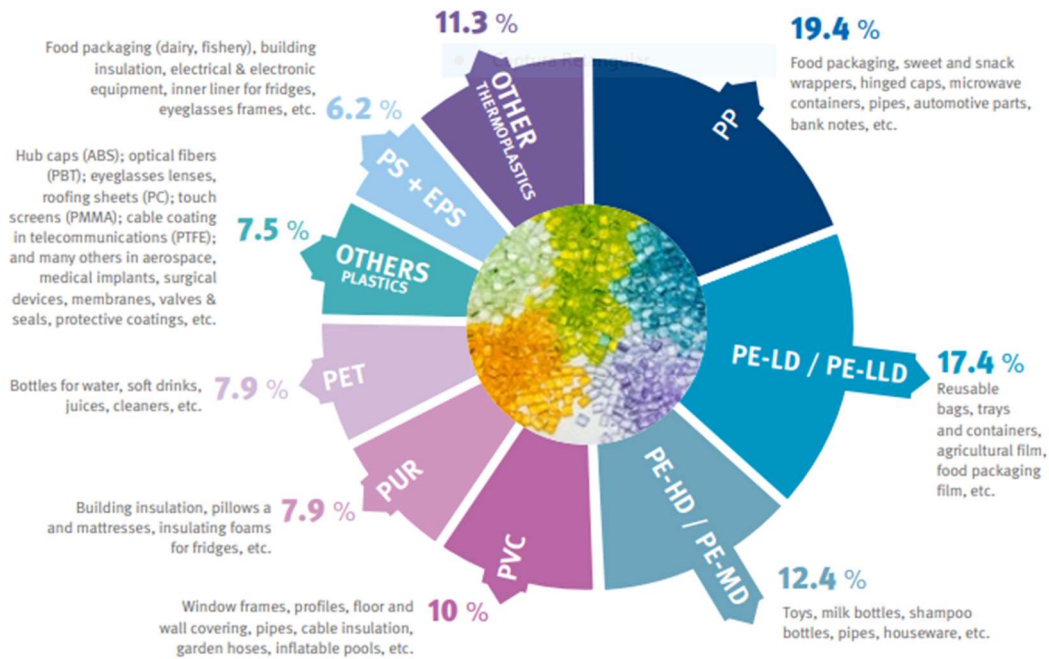


Figure 5. Percentages of the main plastics consumed in European Union and some applications of each one of them, image extracted from “The Facts – Plastics Europe 2020”, a study developed by the Plastic Europe-Association of Plastics Manufactures [15].

### 3 MATERIALS AND METHODS

#### 3.1 REACTANTS AND EQUIPMENTS

Reactants were used to prepare the necessary solutions and to perform analytical methods. They can be distributed according to each experiment in which they were used:

1. Reagents for the production of catalysts used in the synthesis of CNTs:
  - Aluminium oxide, BASF. Formula:  $\text{Al}_2\text{O}_3$ ;
  - Ethanol Absolute (99.99%), Fisher Chemical. Formula:  $\text{C}_2\text{H}_5\text{OH}$ ;
  - Ethylene glycol (99%), Fisher Chemical. Formula:  $\text{C}_2\text{H}_6\text{O}_2$ ;
  - Iron (II) chloride tetrahydrate, Acros Organics. Formula:  $\text{FeCl}_2 \cdot 4\text{H}_2\text{O}$ ;
  - Iron (III) chloride hexahydrate, VWR Chemicals. Formula:  $\text{FeCl}_3 \cdot 6\text{H}_2\text{O}$ .
2. Synthesis of carbon nanotubes and washing:
  - High-density polyethylene (HDPE), melt index 2.2 g/10 min, Sigma-Aldrich. Formula:  $[\text{C}_2\text{H}_4]_n$ ;
  - Low-density polyethylene (LDPE), weight average molecular weight  $\sim 35,000$ , number average molecular weight  $\sim 7,700$ , Sigma-Aldrich. Formula:  $[\text{C}_2\text{H}_4]_n$ ;
  - Polypropylene (PP), weight average molecular weight  $\sim 250,000$ , number average molecular weight  $\sim 67,000$ , Sigma-Aldrich. Formula:  $[\text{C}_3\text{H}_6]_n$ ;
  - Sulfuric acid (95%), VWR Chemicals. Formula:  $\text{H}_2\text{SO}_4$ .
3. Reagents for oxidation runs:
  - Quinoline ( $\text{C}_9\text{H}_7\text{N}$ ), 98% of purity, liquid state, CAS 91-22-5, provided by Alfa Aesar;
  - Isooctane ( $\text{C}_8\text{H}_{18}$ , 2,2,4-trimethyl pentane), 99,9% of purity, CAS 540-84-1, provided by VWR Chemicals;
  - Sulfuric acid ( $\text{H}_2\text{SO}_4$ ), 98% of purity, CAS 7664-93-9, provided by Labkem;
  - Hydrogen peroxide ( $\text{H}_2\text{O}_2$ ), 30% of purity, CAS 7722-84-1, provided by VWR Chemicals;
  - Carbon nanotube, HWCNT, multiwall carbon nanotube, provided by Sigma Aldrich;
  - Ultrapure water.

4. Reagents for the preparation of calibration curves to analyze the concentration of quinoline by UV-VIS spectrophotometry:
  - Ethanol absolute ( $C_2H_5OH$ ), 99,8% of purity, CAS 64-17-5, provided by Fisher Chemical.
  
5. Reagents for the preparation of calibration curves to analyze the concentration of quinoline by HPLC:
  - Acetonitrile ( $C_2H_3N$ ), 99,9% of purity, CAS 75-05-8, provided by Fisher Chemical;
  - Orthophosphoric acid, CAS 7664-38-2, provided by Fisher Chemical;
  - Sodium hydroxide ( $NaOH$ ), 99,2% of purity, CAS 1310-73-2, provided by VWR Chemicals.
  
6. Reagents for the preparation of calibration curves to analyze the quantity of hydrogen peroxide:
  - Titanium (IV) oxysulfate solution ( $TiOSO_4$ ), CAS 13825-74-6, provided by Sigma-Aldrich;
  - Sulfuric acid ( $H_2SO_4$ ), 98% of purity, CAS 7664-93-9, provided by Labkem.

Equipments used during the experiments are identified below.

- HPLC (High-performance liquid chromatography) with a column of specification “NUCLEOSIL 100-5C18” (15cm x 2.1mm) and coupled equipment provided by Jasco: PU-2089 Plus Quaternary Gradient Pump, LC-NET II/ADC, and UV-2075 Plus Intelligent UV/VIS Detector;
- UV-VIS Spectrometer, model T70, provided by PG Instrument Ltd;
- Magnetic stirrers, model C-MAG HS 7, provided by IKA;
- Thermometer, model ETS-D5, provided by IKA;
- Bath shaker, provided by OVAN;
- Oven (drying and heating chambers) provided by BINDER;
- Fume hood with a control flow provided by ECRO CE;

- TOC-L total organic carbon analyzer with the ASI-L autosampler, and with the TNM-L total nitrogen measuring unit, all of them were provided by SHIMADZU.
- FT-IR Spectrometer, model Spectrum Two, provided by PerkinElmer.

### 3.2 SYNTHESIS OF CNTs

The carbon nanotubes applied in this work were all synthesized in a previous master thesis work (Figure 6), which had as main goal the synthesis and characterization of those carbon materials. In the present work the focus is the application of those CNTs in biphasic system oxidation process. Even so, the methodology used to produce the CNTs is exposed in the following.

The CNTs were synthesized via chemical vapor deposition (CVD) over an iron-based catalyst supported in alumina ( $\text{Fe}/\text{Al}_2\text{O}_3$ ). For this purpose, the catalyst  $\text{Fe}/\text{Al}_2\text{O}_3$  was synthesized by a sol-gel methodology. 10 mmol of  $\text{FeCl}_2$  was dissolved in 20 mL of ethanol and heated until reaching its boiling point. 20 mmol of  $\text{FeCl}_3$  was dissolved in 80 mL of ethylene glycol and heated to 60 °C for 5 min. Both solutions were then inserted into an ice bath until reaching temperature equilibrium. The solutions were mixed in one beaker with  $\text{Al}_2\text{O}_3$  (6.6 g), and the mixture was heated to 60 °C for 2 h in a heating plate with stirring. Then, the temperature was increased to 120 °C and the mixture was left at this temperature until reaching a gel-like texture. The temperature was then increased to 200 °C until reaching a powder texture. The obtained powder was subjected to a thermal treatment under nitrogen flow at 300 °C for 12 h and 600 °C for 24 h, leading to  $\text{Fe}/\text{Al}_2\text{O}_3$ .

The CVD process took place in a vertical oven (TH/TV, Termolab) considering LDPE, HDPE, PP and a mixture (MIX) of the three polymers, as carbon source. The mixture of three polymers consisted of 35:25:40 of LDPE:HDPE:PP (mass basis). The oven has an upper and a lower crucible and three regions of temperature control ( $T_1$ ,  $T_2$ , and  $T_3$ ). For the synthesis of CNTs, 1 g of the catalyst was loaded in the lower crucible and 5 g of the desired polymer (or mixture of polymers) on the upper crucible. The synthesis was conducted at  $T_3 = 800$  °C with 1 h hold time upon reaching the desired temperature, under a nitrogen atmosphere ( $40 \text{ mL min}^{-1}$ ). One CNT sample derived from LDPE was also synthesized at  $T_3 = 600$  °C.

After synthesis, the CNT was subjected to acid washing to reduce the quantity of the metal catalyst attached to the structure (50% v/v H<sub>2</sub>SO<sub>4</sub>, 140 °C, 3 h, under reflux), as described elsewhere [63]. After cooling down, the material was abundantly washed with distilled water to remove excess acid and then dried in an oven at 60 °C for longer than 12 h. The CNTs were named according to the starting polymer (and temperature for the material synthesized at 600 or 800 °C), as follows: CNT LDPE 600, CNT LDPE 800, CNT HDPE 800, CNT PP 800 and CNT MIX 800.

In addition, a commercial CNT, provided by Sigma Aldrich, was used to be compared with the synthesized CNTs, identified as CNT COMMERCIAL.



Figure 6. Typical look of CNTs synthesized from polymers.

### 3.3 PRELIMINARY TESTS WITH THE OILY PHASE

The fuel representant in this work is the organic solvent isooctane. Thus, some previous analysis with that compound were performed to know its behaviour in the oxidation processes. The operational conditions used are proposed to be used as well in the biphasic oxidation runs.

#### 3.3.1 TRANSFER OF ISOOCTANE TO WATER

A test was performed to observe possible mass transference of isooctane to the aqueous phase, simulating the conditions used in the oxidation runs. For this purpose, 80% isooctane and 20% ultrapure water at pH 3 were mixed in a beaker at (i) ambient temperature without stirring and (ii) 80 °C and vigorous stirring. After 24 h, the aqueous phase was analyzed by determination of TOC to verify if isooctane was soluble under the working conditions.

### 3.3.2 ISOCTANE OXIDATION

Laboratory tests were performed to certify that hydrogen peroxide does not result in isooctane oxidation under the ODN conditions, as the process envisages to selectively oxidize the model contaminant.

The tests were conducted at a water-oil volume ratio (W/O) of 20/80, a pH 3 for the aqueous phase, and the quantity of hydrogen peroxide required for the oxidation runs ( $C_{H_2O_2} = 247$  g/L). Isooctane was first added to the flask, heated up to a temperature of 80 °C, and the oxidizing solution was added (water and  $H_2O_2$ ). The test was carried out for 24 h. Samples were collected at different times: 0, 5, 10, 15, 60, 240, 480 and 1440 min.

In addition, one test was performed with less amount of hydrogen peroxide, ( $C_{H_2O_2} = 24.7$  g/L) and a sample was collected after 24 h. The oxidation of isooctane was evaluated by measuring the TOC of the samples and by Fourier Transform Infrared Spectroscopy (FT-IR).

### 3.3.3 MASS TRANSFER OF QUINOLINE FROM OIL TO WATER

The experiments to assess the mass transfer of quinoline to water considered the ratio W/O = 20/80, pH 3 in the aqueous phase, 250-1000 mg/L of quinoline in the organic solvent, 80 °C and stirring (200 rpm).

The experiments were carried out on a bath shaker provided by OVAN. Initially, different solutions with quinoline concentrations of 250, 500, 750, and 1000 mg/L in isooctane were distributed into four Erlenmeyer flasks, followed by addition of ultrapure water at pH 3 into each one of them.

Samples were collected during 8 h of the experiment at the following selected times: 0, 5, 10, 15, 60, 240 and 480 min. The samples were withdrawn maintaining the ratio W/O = 20/80. Aliquots were kept into separated Eppendorf flasks for analysis. Quinoline concentration in both phases was monitored by UV/VIS spectrophotometry.

### 3.4 ANALYTICAL METHODS

#### 3.4.1 UV/VIS

UV-VIS Spectrophotometry with a quartz cell of size 10 x 10 mm was used to determine the concentrations of H<sub>2</sub>O<sub>2</sub>, quinoline in aqueous and oily phase and aromatics. H<sub>2</sub>O<sub>2</sub> was determined as in previous works [77]. Briefly, a reaction sample was mixed with TiOSO<sub>4</sub> and H<sub>2</sub>SO<sub>4</sub> 0.5 M. The resulting solution was read at 405 nm. Aromatic compounds were estimated by diluting the reaction samples with a phosphate-buffer solution (pH 7) and measured at 254 nm. Quinoline concentration was estimated at 313 nm, both for aqueous and oily phases. In oily phase, dilutions were made using absolute ethanol.

#### 3.4.2 HPLC

HPLC (High-performance liquid chromatography) was used to identify quinoline in the aqueous medium. For this method, a column “NUCLEOSIL 100-5C18” (15cm x 2.1mm) and a mobile phase with 20% of acetonitrile and 80% of buffer solution, made with orthophosphoric acid (1 mL/L) and adjusted to the pH of 6.5 with sodium hydroxide, were used. All the analysis were done in an isocratic system at a flow of 0.5 mL/min. Quinoline was detected at a wavelength of 313 nm.

#### 3.4.3 pH ANALYSIS

The pH analysis was done right after the end of the oxidation runs, considering that all the aqueous medium used during the work laboratory was adjusted to pH 3, which is known to be the optimum pH for hydrogen peroxide in oxidation [44].

#### 3.4.4 TOTAL ORGANIC CARBON ANALYSIS

Total organic carbon (TOC) analysis was performed by the equipment provided by SHIMADZU with an aliquot of reaction diluted to 10 mL in a volumetric flask.

### 3.4.5 FT-IR

Isooctane samples were analyzed by Fourier Transform Infrared Spectroscopy (FT-IR). The FT-IR spectra was obtained within the range of wavenumber in the analysis from 450 to 4000  $\text{cm}^{-1}$ . All measurements were done at room temperature, with liquid samples.

## 3.5 ADSORPTION OF QUINOLINE

The adsorption experiments followed the same operational conditions used in biphasic oxidation.

### 3.5.1 IN OILY PHASE

20 mL of 1000 mg/L quinoline solution in isooctane was placed in Erlenmeyer flasks. The flasks were placed in bath shaker, provided by OVAN, at 80 °C and stirred at 200 rpm. Upon reaching the temperature, the adsorbent ( $C_{\text{CNT}} = 2.5 \text{ g/L}$ ) was added, considering this as  $t = 0 \text{ min}$ . Adsorption runs were monitored for 8 h, and samples were collected at 0, 1, 4 and 8 h and analysed by UV/Vis.

### 3.5.2 IN A BIPHASIC MEDIUM

60 mL of quinoline solution with a concentration of 1000 mg/L in isooctane was added to the flask, and heated up until temperature reaches 80 °C. Then, 15 mL of ultrapure water at pH 3 was added (O/W=80/20) and, after 2 min under stirring, the CNTs were added in the system with a concentration of 2.5 g/L. Samples were collected from the reaction medium (oily and aqueous phase) periodically to monitor the adsorption. Appropriate volumes of each phase were collected in order to maintain the volumetric ratio of oil-water of 80/20. Samples were analysed by UV/Vis.

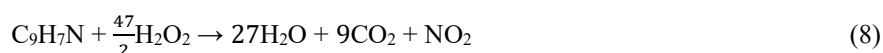
## 3.6 OXIDATION OF QUINOLINE

The oxidation of quinoline using hydrogen peroxide was studied in aqueous solutions and in the biphasic media consisting of isooctane and ultrapure water to simulate fuel treatment.

### 3.6.1 OXIDATION IN AQUEOUS PHASE

The oxidation tests were performed in the aqueous phase (CWPO) with ultrapure water at pH 3, H<sub>2</sub>O<sub>2</sub>, the selected CNT as a catalyst, and quinoline.

The ratio between the oxidant and the contaminant was 10 times the quantity of oxidant mol necessary to mineralize completely quinoline. In this way, the calculations were based on the stoichiometric equation of mineralization of quinoline, which is shown in Equation (8). The concentration of H<sub>2</sub>O<sub>2</sub> needed was determined as C = 6.2 g/L.



The experiments were performed in a round-bottom glass flask immersed in a silicone bath, as represented in Figure 7. Silicone bath was set at 80 °C and 50 mL of 100 mg/L quinoline solution in ultrapure water at pH 3 was loaded in the round-bottom flask. Upon reaching 80 °C, H<sub>2</sub>O<sub>2</sub> was added in the system, followed by the addition of the catalyst ( $C_{\text{CNT}} = 2.5 \text{ g/L}$ ). The reaction was monitored by withdrawing samples at 0, 15, 30, 60, 120, 240, 360, 480 and 1440 min. The samples were immediately submerged in an ice bath for the following analysis. Quinoline concentration was monitored via HPLC, and H<sub>2</sub>O<sub>2</sub> concentration was determined via UV/VIS.



Figure 7. Setup for oxidation experiments.

At the end of the reaction, the catalyst and reaction medium were separated by filtration. The liquid was also analyzed by TOC, pH and aromatics. Additionally, a non-catalytic run (N.C) was also carried out, under the same protocol, with the exception of the presence of the catalyst.

### 3.6.2 BIPHASIC OXIDATION

Biphasic oxidation experiments were carried out under similar conditions as for the oxidation in aqueous medium (80 °C,  $C_{CNT} = 2.5$  g/L, considering the total volume of reaction). The reaction volume consisted of 80 mL of 1000 mg/L quinoline solution in isooctane, and 20 mL of an aqueous  $H_2O_2$  solution at pH 3 (8.4 mL of 60%  $H_2O_2$  completed to 20 mL with ultrapure water, resulting in a  $C_{H_2O_2} = 247$  g/L). The volume of the samples withdrawn from each phase were done respecting the volume ratio of oil-water of 80/20.  $H_2O_2$  and quinoline in the aqueous phase were measured via UV/VIS and HPLC, respectively. Quinoline in the oily phase was measured by UV/VIS.

By the end of the reaction (Figure 8), the reaction medium was filtered to collect the catalyst, and the liquid was centrifugated to separate aqueous and oily phase. The aqueous phase was analyzed by TOC, pH and aromatics, and the oily phase had the aromatic concentration calculated.



Figure 8. Final product of biphasic oxidations.

## 4 RESULTS AND DISCUSSION

### 4.1 PRELIMINARY TESTS ON OILY PHASE

Some tests were performed with the organic phase to know its behaviour and possible interferences in the system, such as evaporation (to maintain the initial ratio between phases) and the transfer of isooctane to water (to know a possible interference of organic load in the aqueous phase from isooctane). Furthermore, oxidation tests were also performed to ensure the selective oxidation of the contaminant.

#### 4.1.1 TRANSFER OF ISOOCTANE TO WATER

TOC was determined in aqueous aliquots withdrawn from the biphasic systems (W/O = 20/80) carried out under different operational conditions. The first was carried out under stirring at 80 °C for 24 h, without contaminant or oxidant. The second considered the same ratio W/O = 20/80 and was left at room temperature without stirring for 24 h. Both of them had a total volume of 100 mL. The TOC values found were 10.86 mg/L and 0 mg/L, respectively.

Based on those results, the theoretical TOC can be calculated, assuming the percentage of the resultant values per the possible total oxidation of the organic phase. Considering the molar mass (114.23 g/mol) and the density (692.5 g/L) of isooctane, the higher value of TOC (10.86 mg/L) represented 0.002% of the total organic carbon possible to be detected. This value is thus too low to be considered a damage interference in the oxidation process. Lastly, it can be observed that the temperature and stirring promotes the transfer of isooctane to water since the measured TOC at room temperature and stirring has a value close to zero.

#### 4.1.2 ISOOCTANE OXIDATION

As the main goal of this work is to accomplish selective oxidation, hydrogen peroxide should oxidize only the contaminant. Thus, some preliminary oxidation tests were performed with the isooctane organic phase to analyze any possible oxidation of this component.

From analysis of Figure 9 it is possible to observe that number of organic compounds in the aqueous phase increased only 9% between 10 min and 24 h of run.

After 24 h of run, the TOC value was 62.6 mg/L of organic compounds in the aqueous phase, representing only 0.013% of the theoretically possible.

Another test using a different load of  $\text{H}_2\text{O}_2$  ( $C_{\text{H}_2\text{O}_2} = 24.7 \text{ g/L}$ ) had a resultant TOC of 53.4 mg/L after 24 h of run. In conclusion, the oxidant concentration won't be the main parameter for possible isooctane oxidation.

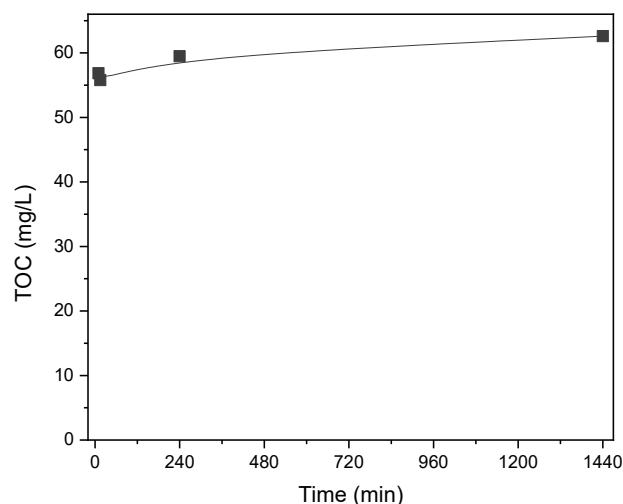


Figure 9. Isooctane oxidation test during 24 h (80 °C, pH 3, W/O = 20/80,  $C_{\text{H}_2\text{O}_2} = 247 \text{ g/L}$ ). The lines are only intended to guide the eyes.

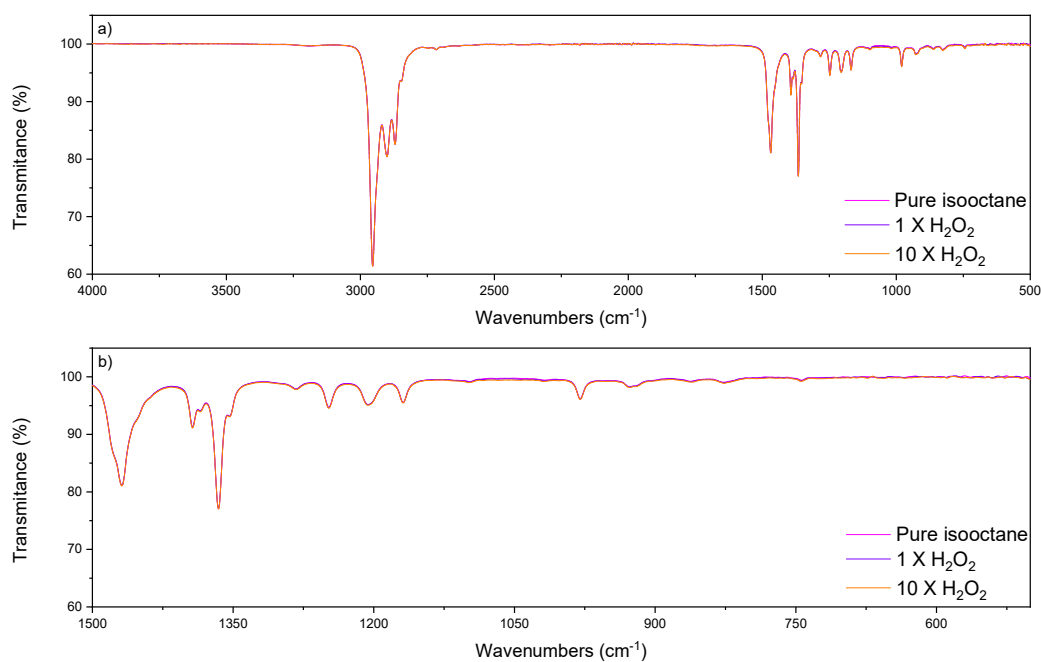


Figure 10. FT-IR spectra of pure isooctane in comparison with isooctane samples after oxidation reactions: a) complete and b) fingerprint spectra.

Moreover, FT-IR analyses were done with those two samples with different oxidant concentration after 24 h of run and compared with the isooctane spectra of pure solvent (99.9%).

Figure 10 shows that the isooctane samples didn't suffer significant alteration or changes, FT-IR spectra in practice overlapping. It is thus concluded that isooctane holds the same structure after the oxidation reactions without a loss of properties.

#### 4.1.3 MASS TRANSFER OF QUINOLINE

A preliminary test was performed to decide which would be the most appropriate concentration of quinoline in the oily phase, in a concentration range from 250 to 1000 mg/L. The goal was to analyze which concentration would present the least mass transference from the oily phase containing quinoline to the aqueous phase.

In Figure 11, the data show the  $\mu\text{mol}$  of quinoline along time in both oily and aqueous phases. It can be observed that the initial behavior between the first collection time until 60 minutes of run represents almost the same result as the final value after 8 h of experiment, except for the run with 250 mg/L of quinoline in the oily phase.

As observed, for the two lower concentrations of quinoline, 250 and 500 mg/L, the relative quantity of quinoline transferred from oil to water was the highest among the tests performed, 41% and 15% of the initial contaminant present in the aqueous phase, respectively. The final quinoline transferred in the tests with quinoline solutions of 750 and 1000 mg/L represented 7% of transference in both of them.

However, the higher the concentration of quinoline in the oily phase, the higher is the quinoline amount at the end of the runs in the aqueous phase. For example, in the run with 1000 mg/L (d), there are 0.18  $\mu\text{mol}$  of quinoline in the aqueous phase, while in the run with 250 mg/L (a), there are 0.01  $\mu\text{mol}$  of contaminant after 8 h in the aqueous phase. As the work intends to develop an efficient oxidation system to remove quinoline from the oily phase, to properly assess the effect of oxidation in the studied process rather than the effect of mass transfer, biphasic oxidation runs with 1000 mg/L of quinoline solutions were selected for further studies.

Moreover, when a polar organic compound dissolved in an organic solvent is in contact with an immiscible aqueous solvent, the component will distribute itself between the two phases depending on pH, salinity and ionic strength in the water phase [77]. The

ratio between the organic compound amounts in the oily and aqueous phase is called partition coefficient.

As an example, the value of 3.5 was found in another study for the partition coefficient of quinoline in an oily/aqueous system with groundwaters and tar oil. The operational conditions were 6.6-7.2 of pH and the contaminant concentrations between 300 and 1300 mg/L [78].

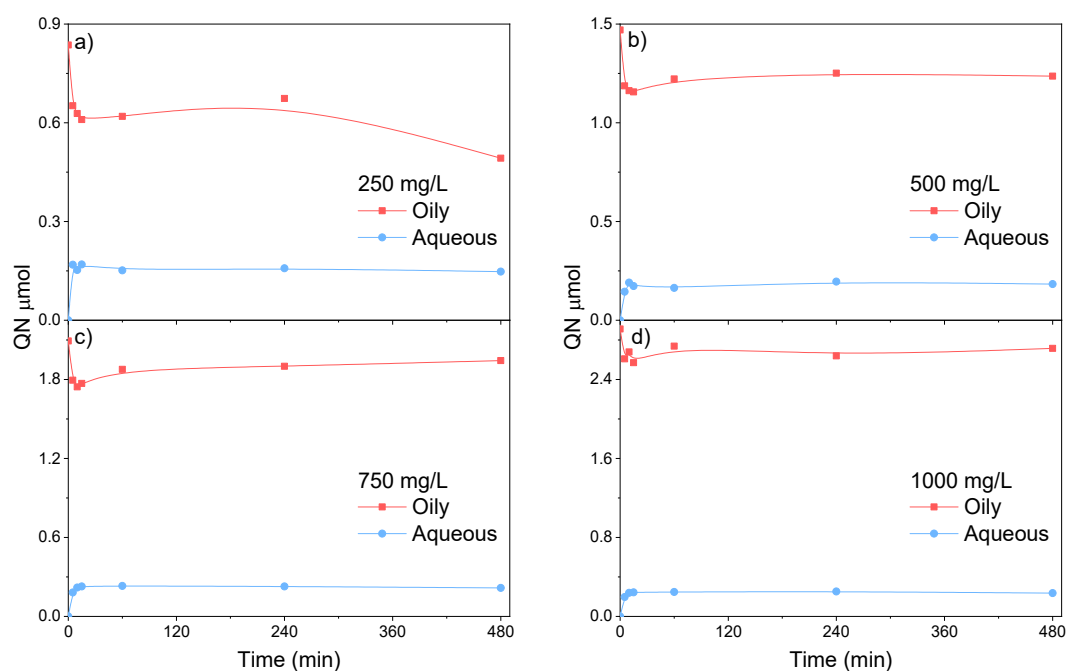


Figure 11. Mass transfer of quinoline into the aqueous phase from oily phase (W/O = 20/80) at different concentrations: (a) 250, (b) 500, (c) 750 and (d) 1000 mg/L (80 °C, pH 3 in aqueous phase). The lines are only intended to guide the eyes.

## 4.2 DEVELOPMENT OF ANALYTICAL TECHNIQUES

Due to the exploratory nature of the present work, analytical techniques had to be developed. The next topics will explain how the calibration curves was built to measure the concentration of quinoline, H<sub>2</sub>O<sub>2</sub> and aromatic compounds.

### 4.2.1 DETERMINATION OF H<sub>2</sub>O<sub>2</sub> CONCENTRATION

Hydrogen peroxide solutions with different concentrations were prepared to obtain the calibration curves needed to analyze the dissociation of hydrogen peroxide during the reactions.

Two calibration curves were considered to estimate the concentration of hydrogen peroxide in the aqueous aliquots during the reactions. One calibration curve for the samples taken in the CWPO reactions of quinoline carried out in aqueous solutions with an initial concentration of 100 mg/L of quinoline. Another calibration curve was used to analyze the aqueous phase in biphasic oxidation reactions carried out with an initial concentration of 1000 mg/L of quinoline in the oily phase.

The methodology to determine  $\text{H}_2\text{O}_2$  concentration during the CWPO runs was based on the following steps: first, collecting 0.1 mL of the reaction medium and diluting with distilled water in a 20 mL volumetric flask containing 1 mL of  $\text{H}_2\text{SO}_4$  (0.5 M) and 0.1 mL of  $\text{TiOSO}_4$ . After that the samples were analyzed by UV-VIS spectrophotometry at the wavelength of 405 nm to determine their absorbance. Figure 12 presents the calibration curve with an  $\text{H}_2\text{O}_2$  concentration range from 500 to 6200 mg/L, the equation found by the linear regression, and the value of  $R^2$ , showing a good adjustment to the calibration curve.

The determination of  $\text{H}_2\text{O}_2$  concentration for the biphasic oxidation runs with an initial concentration of quinoline of 1000 mg/L was done using the second hydrogen peroxide calibration curve, which is shown in Figure 13. To analyze the concentration of hydrogen peroxide, an aliquot of 0.1 mL of the reaction medium is collected and diluted with distilled water in a 20 mL volumetric flask. Another aliquot of 0.7 mL was taken to this volumetric flask and diluted with distilled water in a 20 mL volumetric flask containing 1 mL of  $\text{H}_2\text{SO}_4$  (0.5 M) and 0.1 mL of  $\text{TiOSO}_4$ . Similar to the previous, samples were analyzed by UV-VIS spectrophotometry at the wavelength of 405 nm to determine their absorbance.

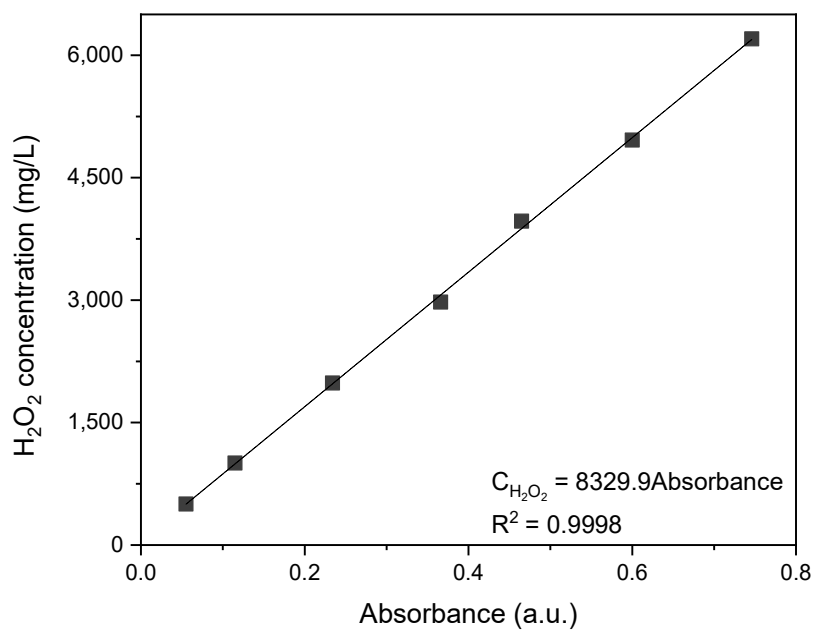


Figure 12. Calibration curve for the determination of H<sub>2</sub>O<sub>2</sub> concentration in the CWPO experiments carried out with 100 mg/L of quinoline in aqueous solution.

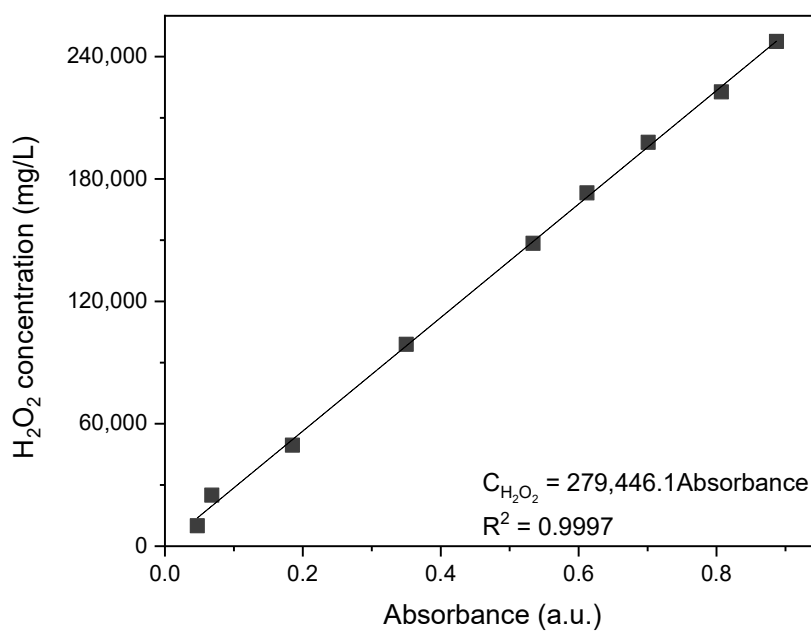


Figure 13. Calibration curve for determination of H<sub>2</sub>O<sub>2</sub> concentration in the experiments carried out with quinoline concentration of 1000 mg/L.

In Figure 13 it is possible to observe that the  $H_2O_2$  concentration range from 10,000 to 250,000 mg/L and that the equation found by the linear regression and the value of  $R^2$ , also represents a good fitting to the calibration curve.

#### 4.2.2 DETERMINATION OF QUINOLINE CONCENTRATION BY SPECTROPHOTOMETRY

##### 4.2.2.1 DETERMINATION OF QUINOLINE IN OILY PHASE

Solutions with different concentrations of quinoline in isooctane were prepared and analyzed by UV/VIS spectrophotometry using the selected wavelength of 313 nm. That was the wavelength with the major absorbance by the quinoline spectra and also the chosen value by other studies with quinoline [37, 79]. The concentration range of quinoline was from 1 to 50 mg/L, these values were decided taking into consideration the absorbance values in this range, which are better closer to the limits from 0 to 1 a.u of absorbance.

The calibration curve for determination of quinoline concentration in isooctane is presented in Figure 14, where is also presented the equation obtained by the linear regression and the value of the  $R^2$ , showing the good fitting of the experimental data.

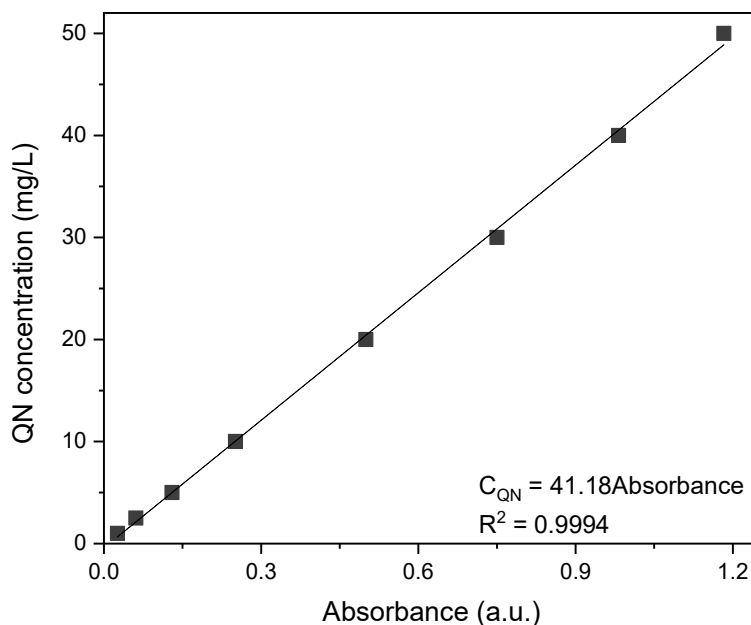


Figure 14. Calibration curve for the determination of quinoline concentration in isooctane solutions.

As isooctane is a noxious organic solvent, a test was made using ethanol, a more environmentally friendly solvent, to perform the dilutions of quinoline solution samples, aiming to avoid the usage of higher amount of isooctane. To assess this possibility, a mixture was done to test the two solvents' miscibility, being concluded that they are miscible, allowing to take reaction aliquots from a reaction performed with isooctane, and further dilute it with ethanol, since these two solvents are miscible.

Following the same steps, quinoline spectrum was obtained using ethanol as solvent, the same wavelength with the major absorbance being chosen and presented in Figure 15 (313 nm). The calibration curve for determination of quinoline concentration, obtained with the solutions prepared using ethanol as solvent, are plotted in Figure 16, followed by the linear regression equation and the  $R^2$ .

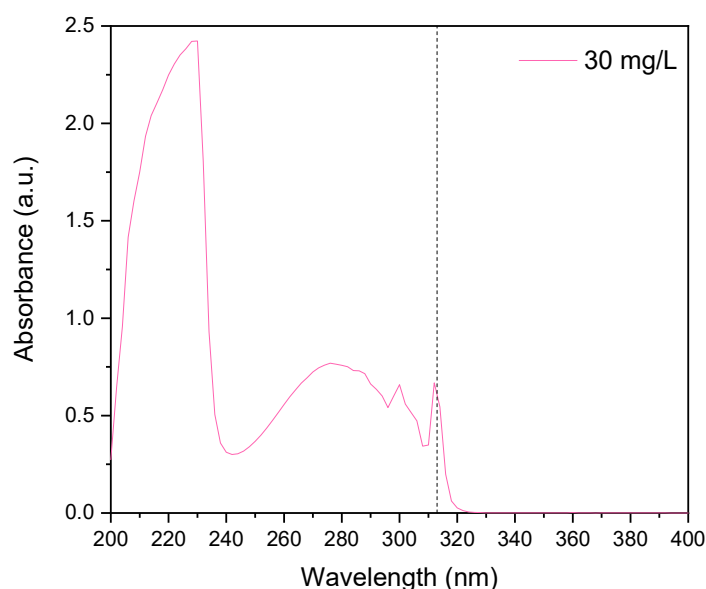


Figure 15 - Spectra of quinoline in ethanol.

In addition, when ethanol was used to make the dilutions, the absorbance value was higher than those measurements done without ethanol, meaning that the sensibility of the analysis is higher, less quantity of sample from the reaction medium being necessary to determine the concentration of quinoline using ethanol solutions.

The calibration curve performed using ethanol as solvent was selected for the next experiments, and ethanol was used for the dilutions in an oily medium.

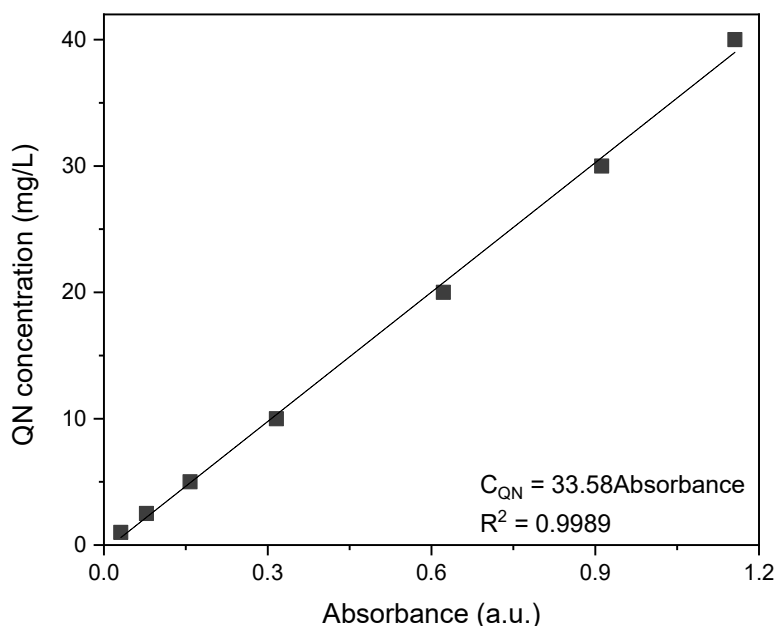


Figure 16. Calibration curve for the determination of quinoline concentration in isooctane solutions diluted with ethanol.

#### 4.2.2.2 DETERMINATION OF QUINOLINE IN AQUEOUS PHASE

The 100 mg/L quinoline aqueous solution, at pH 3, was analyzed by UV/VIS spectrophotometry from 200 to 800 nm and the higher wavelength was chosen as reference. The most interesting peak was found at 313 nm, which had the major absorbance, as shown in Figure 17a.

In addition, the highest possible concentration of quinoline to measure by this analytical technique was 40 mg/L, because of the absorbance value, keeping close to the limits from 0 to 1 a.u. of absorbance.

The calibration curve for determination of quinoline concentration in an aqueous medium, as well as the equation generated by the linear regression and the value of  $R^2$ , are presented in Figure 18.

However, the determination of quinoline concentration calculated based on the calibration curve of Figure 18 can be affected by some interferences from other compounds. For instance, in the graph of Figure 17b it is shown that hydrogen peroxide spectrum can also absorb in the wavelength of 313 nm.

The different concentrations in Figure 17 analyzed the interference of various amounts of quinoline or  $H_2O_2$  in their spectrum. A model hydrogen peroxide solution was

prepared with the amount of oxidant used in the biphasic oxidation. And the first dilution (7423 mg/L) was 0.15 mL in a 5 mL volumetric flask, which was the same volume that would take from the biphasic oxidation to the analysis. The following hydrogen peroxide concentrations were to analyse the differences in the spectrum by the increase of the concentration.

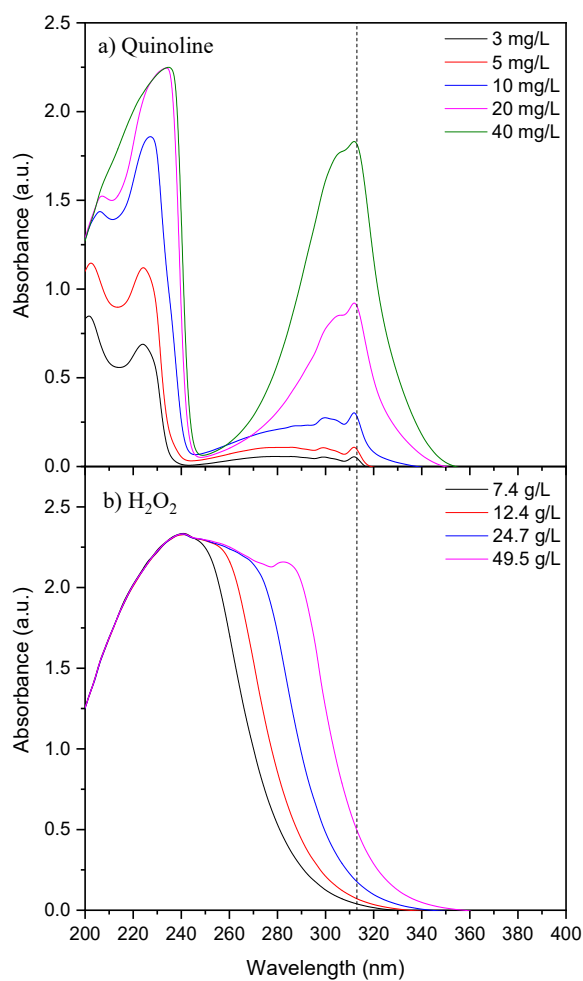


Figure 17. Spectra from different concentration of (a) quinoline aqueous solution and (b) H<sub>2</sub>O<sub>2</sub>.

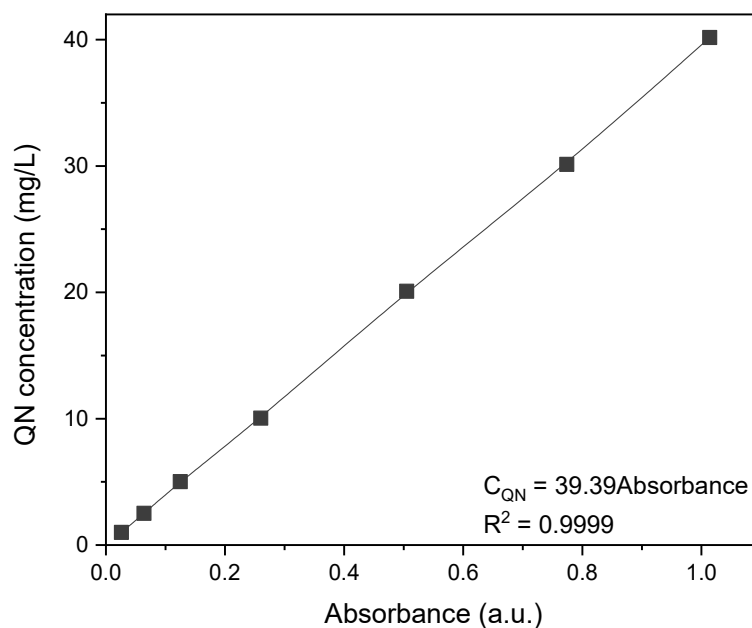


Figure 18. Calibration curve of quinoline in aqueous medium by UV/VIS.

Due to the interference of  $\text{H}_2\text{O}_2$ , another calibration curve with the different  $\text{H}_2\text{O}_2$  concentrations used in the biphasic oxidations was built for UV/VIS spectrophotometry analysis at the wavelength of 313 nm, as depicted in Figure 19. That last calibration curve was used to discount the absorbance of  $\text{H}_2\text{O}_2$  (its interference) to the measurement of quinoline in the aqueous phase.

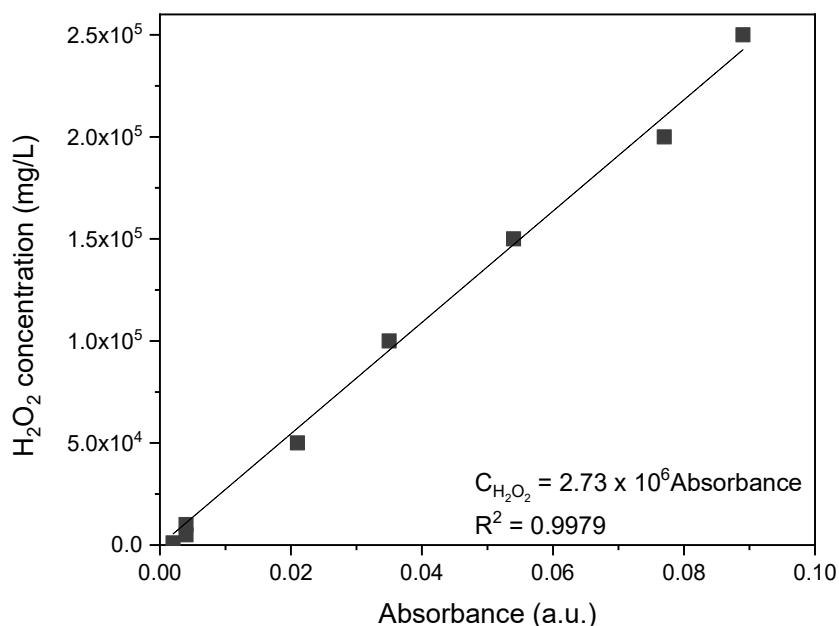


Figure 19. H<sub>2</sub>O<sub>2</sub> concentration in the wavelength of 313 nm.

Thus, the quantity of quinoline in the aqueous phase was calculated by the calibration curve of Figure 18, discounting the amount of H<sub>2</sub>O<sub>2</sub> in each of the collected points, determined by the colorimetric method using TiOSO<sub>4</sub>, as above explained.

#### 4.2.3 DETERMINATION OF QUINOLINE CONCENTRATION BY HPLC

The wavelength used to measure the peak absorbance of the compounds was 313 nm, and the quinoline concentration range from 1 to 100 mg/L based on the aqueous solution concentration used in the CWPO experiments.

The calibration curve with the corresponding equation obtained by linear regression and the value of R<sup>2</sup> for the determination of quinoline concentration in an aqueous medium by HPLC is presented in Figure 20. The value of R<sup>2</sup> was 0.9976, which can be considered a good fitting of the experimental data.

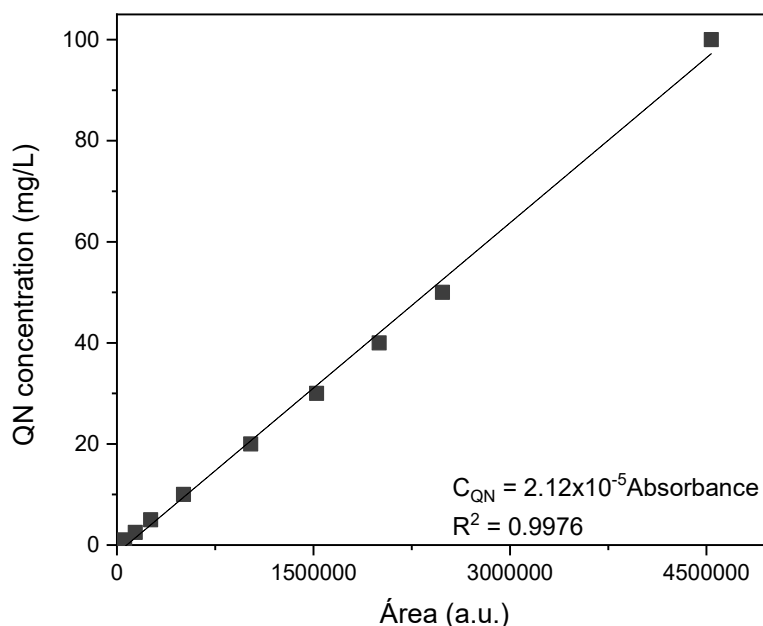


Figure 20. Calibration curve for the determination of quinoline concentration in aqueous solutions by HPLC.

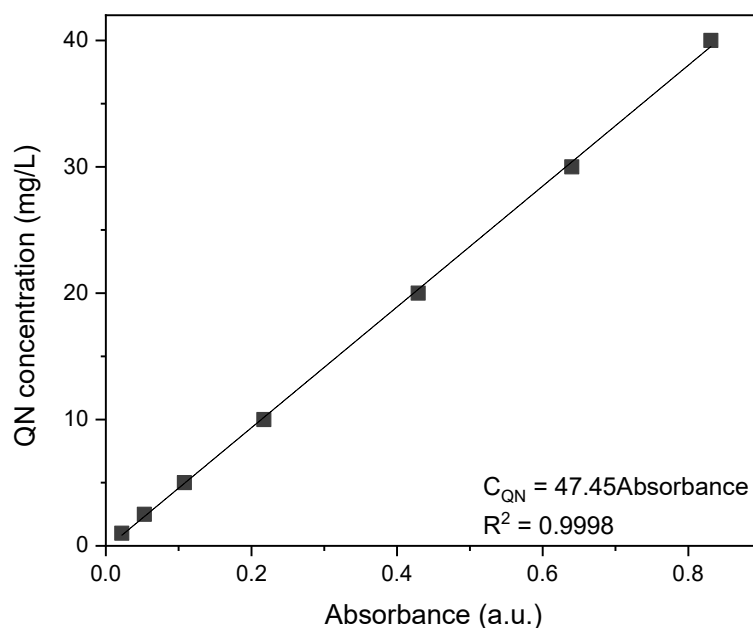
#### 4.2.4 DETERMINATION OF AROMATICS

The aromaticity was measured by two calibration curves, one in an aqueous medium and another in an oily medium, made with quinoline compound in different concentrations and analyzed by UV/VIS spectrophotometry at the wavelength of 254 nm, which is the representing peak of aromatic compounds, as defined in previous works [80]. Both calibration curves have a concentration range from 1 to 40 mg/L.

In the oily medium, the dilutions were performed with ethanol, just like the calibration curve of quinoline in isooctane and ethanol solutions with the difference of the wavelength, which is 254 nm in this present methodology. This calibration curve for aromatics determination is shown in Figure 21, with the linear regression equation and the corresponding  $R^2$ .

In the aqueous medium, the dilutions to the known quinoline concentration were made with a buffer solution with pH 7. In Figure 22 is presented the calibration curve for

aromatics in the aqueous medium, followed by a well-fitted equation and the value of



$R^2$ .

Figure 21. Calibration curve for the determination of aromatics in oily medium as quinoline.

Sample at the end of runs were taken to monitor the aromatic compound in the reactions. In CWPO the samples were of 2.5 mL diluted in volumetric flasks of 5 mL. In the biphasic oxidation for oily phase, the samples were of 0.15 mL while for the aqueous phase, the samples were of 0.2 mL, both of them diluted in volumetric flasks of 5 mL and, posteriorly, analyzed by UV/VIS spectrophotometry.

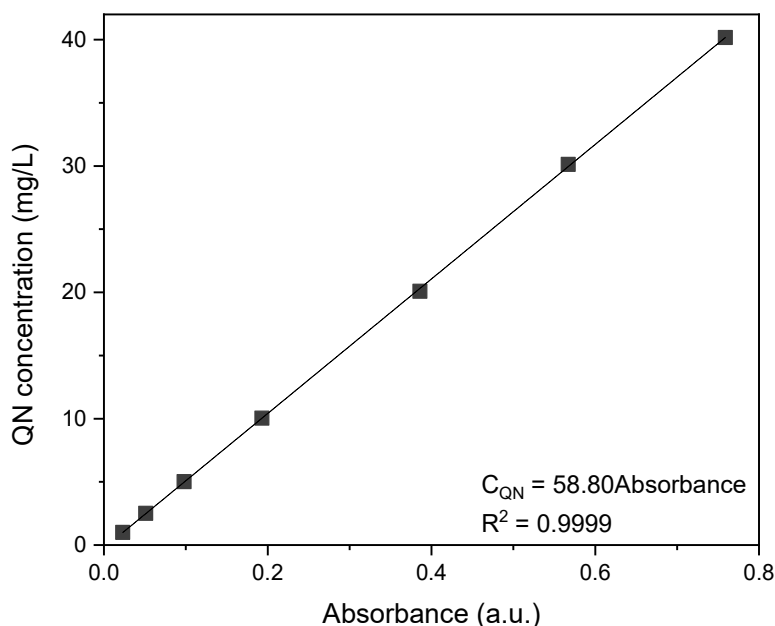


Figure 22. Calibration curve for the determination of aromatic compounds in aqueous medium based on the concentration of quinoline.

### 4.3 ADSORPTION OF QUINOLINE

The adsorption tests were done to analyze the possible adsorption of the model contaminant by the CNTs and to measure the real efficiency of the oxidation process to remove quinoline by oxidation and extraction and not by adsorption.

#### 4.3.1 ORGANIC ADSORPTION

The results of adsorption of quinoline in the organic phase are shown in Figure 23, with all the different CNTs tested.

Most of the CNTs presented similar behaviors and finished the test with quinoline concentration close to the initial value. Adsorption accounted for 4, 0, 22, 8, 10 and 0% of quinoline removal from the organic medium in the presence of CNT LDPE 600, CNT LDPE 800, CNT HDPE 800, CNT PP 800, CNT MIX 800 and CNT COMMERCIAL, respectively. It means that the adsorption of the contaminant accomplished by most of the carbon materials can be considered low or negligible.

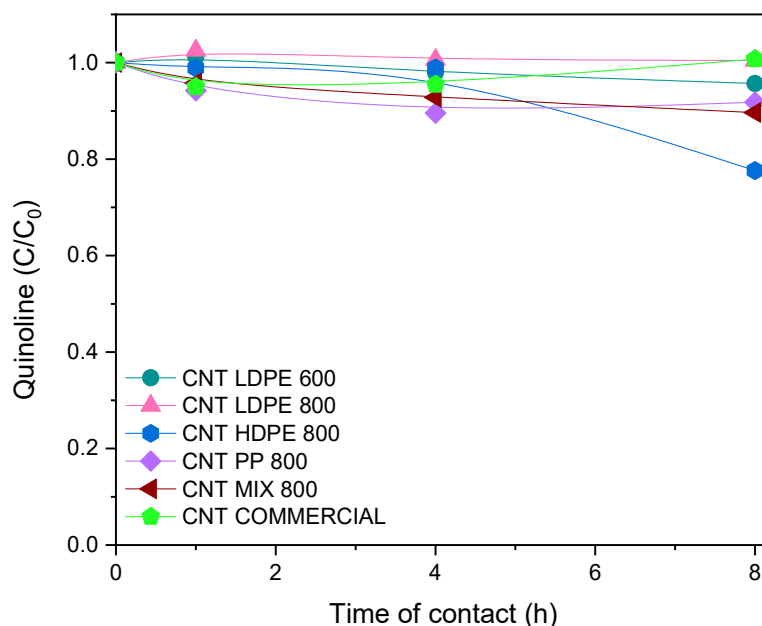


Figure 23. Adsorption of quinoline on the CNTs over contact time (80 °C,  $C_{CNT} = 2,5$  g/L,  $C_{QN} = 1000$  mg/L in isooctane). The lines are only intended to guide the eyes.

#### 4.3.2 BIPHASIC ADSORPTION

After the analysis of the possible organic adsorption by the CNTs in only one phase system, the adsorption was tested in a biphasic system with the quinoline solution in isooctane and ultrapure water with the six different CNTs.

The collected points are shown in Figure 24, which presents the values of quinoline (in mol) in both phases during the eight hours of the run. The process starts with the quinoline being present only in the oily phase. In order to determine amount of adsorbed quinoline, the amount of quinoline in both phases was accounted for.

In the case of the six CNTs used in this experiment, the final result was closer to the organic adsorption, with considerably low adsorption observed by the CNTs. For CNT LDPE 800, CNT HDPE 800, CNT PP 800 and CNT MIX 800, 6% of quinoline was removed by adsorption under a biphasic system. In the presence of CNT LDPE 600, only

2% of quinoline was removed by adsorption. the commercial sample of CNT (CNT COMMERCIAL) resulted in the highest adsorption (12% of quinoline).

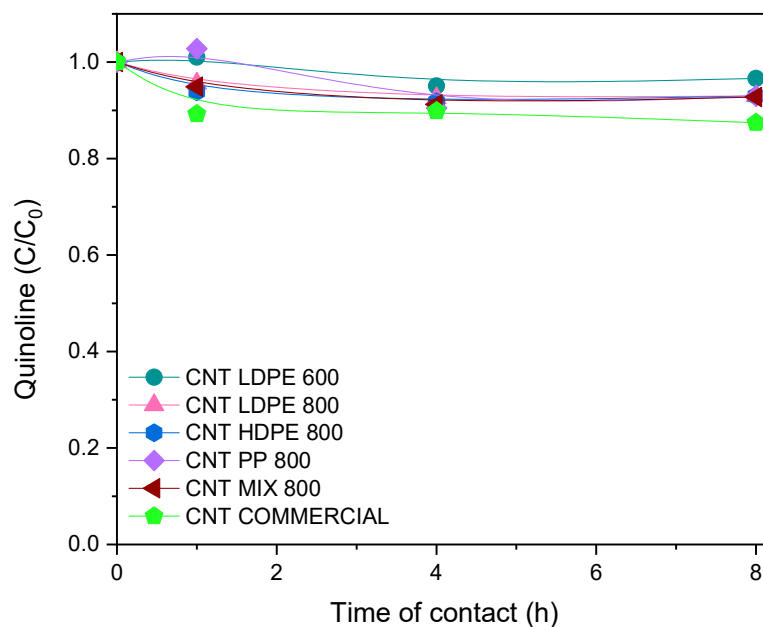


Figure 24. Adsorption of quinoline under a biphasic system (80 °C, W/O = 20/80,  $C_{CNT} = 2.5$  g/L,  $C_{QN,0} = 1000$  mg/L in isoctane). The lines are only intended to guide the eyes.

Figure 25 illustrates an example of an Erlenmeyer with the biphasic system in the adsorption runs, showing that the CNTs had the preference of being in the interphase of the system.

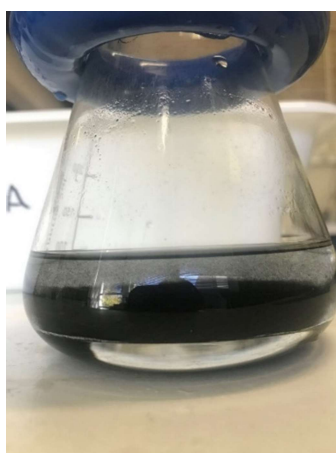


Figure 25. Example of biphasic system in the biphasic adsorption runs.

#### 4.4 CATALYTIC WET PEROXIDE OXIDATION (CWPO)

The CWPO runs done in this work were useful to analyze how each CNT completed the oxidation process without the interphase barrier in a biphasic system as proposed.

##### 4.4.1 CONCENTRATION OF HYDROGEN PEROXIDE IN CWPO RUNS

The analysis of hydrogen peroxide concentration evolution aims to measure its dissociation into radicals during the oxidation process. Considering that it depends mostly on the activity the catalyst, in this case, by the CNTs. Also, a non-catalytic run was performed to compare with the catalytic systems. The results obtained are presented in Figure 26.

As is possible to observe, the non-catalytic run presents the worst efficiency, as expected, with only 6% of degradation at the end of 24 h of the oxidation process. On the other hand, the catalytic runs with different CNTs showed significant degradation. They all accomplished the total degradation of hydrogen peroxide in the system in 24 h of reactions. Although they all resulted in complete decomposition of hydrogen peroxide in 24 h, the kinetics of decomposition was different. The slowest degradation resulted from CNT COMMERCIAL, which after eight hours of run still had 28.9% of hydrogen peroxide remaining in the reaction medium. In the presence of CNT LDPE 600, CNT LDPE 800, CNT HDPE 800, CNT PP 800 and CNT MIX 800, 2, 6, 3, 2 and 5 of H<sub>2</sub>O<sub>2</sub> still remained at 8 h of reaction.

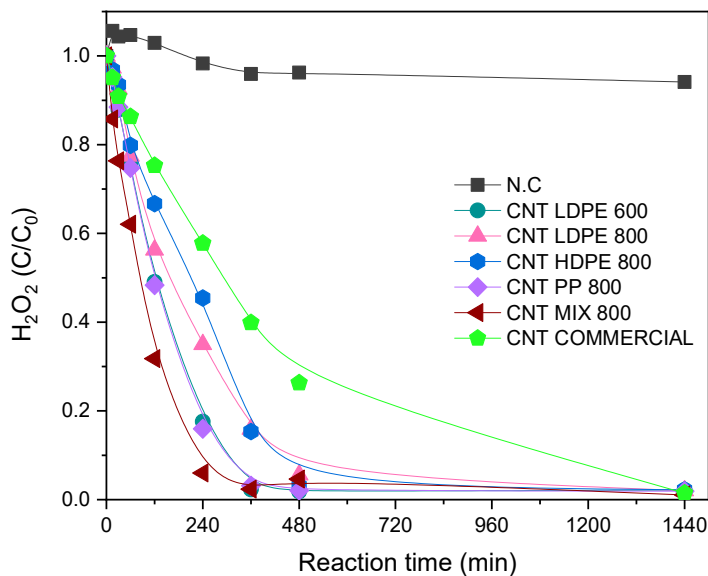


Figure 26. Hydrogen peroxide concentration measured by UV/VIS in CWPO runs (80 °C, pH<sub>0</sub> 3,  $C_{QN}$  = 100 mg/L in water,  $C_{CNT}$  = 2.5 g/L,  $C_{H_2O_2}$  = 6.2 g/L). The lines are only intended to guide the eyes.

Thus, all CNTs derived from polymeric materials resulted in higher decomposition of the oxidant source compared to the N.C and the CNT COMMERCIAL.

#### 4.4.2 CONCENTRATION OF QUINOLINE IN CWPO RUNS

In Figure 27 is shown the normalized concentration of quinoline against time of reaction (min).

Although the runs were performed for 24 hours, all the catalytic runs resulted in total removal of quinoline in less than four hours of experiment. Thus, Figure 27 only shows the data for the first 4 h of reaction. The only exception is for the non-catalytic run, in which quinoline was not totally removed before that time. In the N.C run, even after 24 h, there was still around 3.45% of the initial quinoline concentration, thus pointing out that the catalytic systems result in a much more efficient process.

Among the CNTs, CNT COMMERCIAL presented the slowest degradation of quinoline. After 2 h of oxidation reaction, CNTs prepared in our research group led to quinoline concentrations closer to zero faster than CNT COMMERCIAL.

The faster degradation of the model contaminant was accomplished in the presence of CNT MIX 800, which resulted in a total degradation of quinoline in just 30 minutes of reaction. The remaining CNTs resulted in complete degradation of quinoline

in 120, 240, 60, and 120 min of reaction (for CNT LDPE 600, CNT LDPE 800, CNT HDPE 800 and CNT PP 800, respectively). These results are in line with the  $H_2O_2$  concentrations observed during the run, since as more hydrogen peroxide was dissociated, there was a higher possibility to oxidize the quinoline.

In the presence of CNT MIX 800, after 30 minutes, the concentration of  $H_2O_2$  in the medium was around 72% of its original value (as observed in Figure 26), only 28% of decomposition, and the quinoline concentration was almost zero. That happened due to the proportion of oxidant to contaminant proposed in this work, which was ten times the molar quantity of oxidant needed to mineralize the contaminant. Thus, amount of hydrogen peroxide required to fully degrade quinoline in the organic fraction was only 10% of the oxidant quantity used in this work. That is why, even with a large quantity of oxidant without dissociation in the medium (72%), all the quinoline has been degraded.

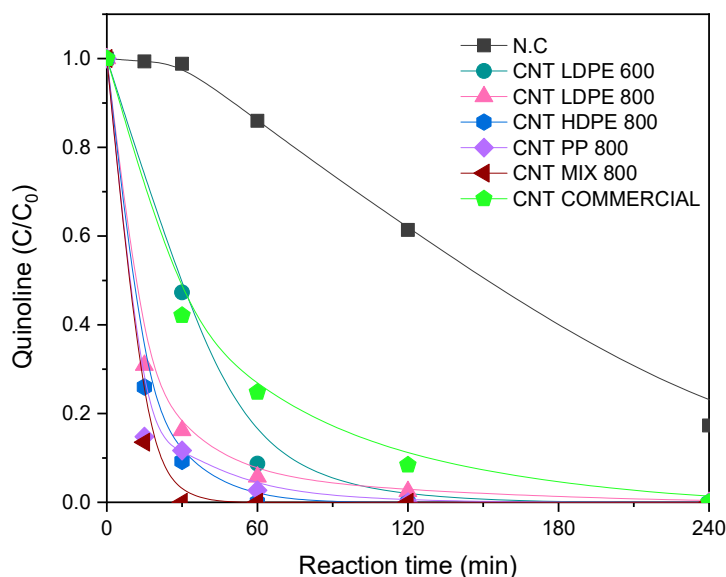


Figure 27. Concentration of quinoline in CWPO runs ( $80\text{ }^{\circ}\text{C}$ ,  $\text{pH}_0\text{ }3$ ,  $C_{\text{QN}} = 100\text{ mg/L}$  in water,  $C_{\text{CNT}} = 2.5\text{ g/L}$ ,  $C_{\text{H}_2\text{O}_2} = 6.2\text{ g/L}$ ). The lines are only intended to guide the eyes.

Besides the quinoline concentration analyzed in the CWPO runs, in the non-catalytic run it was possible to detect the production of some possible reaction intermediates by HPLC (however not identified). The HPLC chromatograms showed other peaks in different retention times than that of quinoline in the analyzed samples. They are presented in Figure 28 and named as Intermediate 1, Intermediate 2, Intermediate 3 and Intermediate 4. The maximum area (and therefore, concentration)

reaches a peak at 2, 6, 6, and 2 h for intermediate 1, 2, 3 and 4, respectively. After reaching their peak, their areas diminish, or they are no longer detected, indicating that they suffer further oxidation.

It was not possible to detect the production of intermediates in other runs, since the quinoline was degraded much faster than in the non-catalytic run. In addition, this quick degradation of the pollutant is probable due to the ratio between the oxidant and the pollutant, which followed the proposed biphasic system conditions. A previous study showed the relation between ratio and contaminant conversion, presenting an improvement with the increase of oxidants in the system [35].

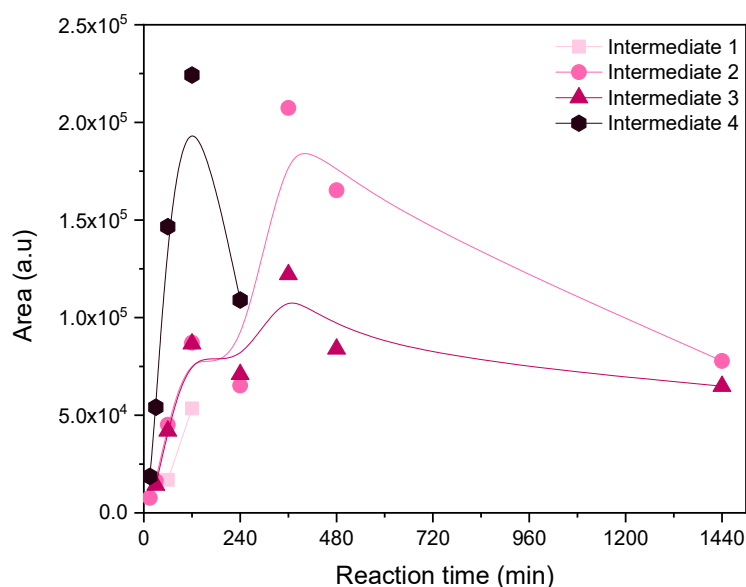


Figure 28. Reaction intermediates identified by the different retention times in HPLC (80 °C, pH<sub>0</sub> 3,  $C_{\text{QN}} = 100$  mg/L in water,  $C_{\text{H}_2\text{O}_2} = 6.2$  g/L). The lines are only intended to guide the eyes.

#### 4.4.3 TOTAL ORGANIC CARBON IN CWPO

The analysis of TOC represents the concentration of carbon in organic compounds present in the medium that has not been mineralized.

The TOC removal obtained at the end of the reactions are shown in Figure 29. Observing the values, it is possible to see that the higher organic concentration in the medium results by the non-catalytic run, with 69.8 mg/L, which corresponds to 88% of the initial TOC. This is in agreement with what was observed in the HPLC analysis: the

non-catalytic run was the only run that allowed to identify compounds other than quinoline.

The catalytic runs reveal significant different results among them. The abatement of TOC was 28, 70, 44, 60, 73 and 34% in the presence of CNT LDPE 600, CNT LDPE 800, CNT HDPE 800, CNT PP 800, CNT MIX 800 and CNT COMMERCIAL, respectively. Thus, the presence of the CNTs resulted in a positive increase in the abatement of TOC compared to the non-catalytic run. Furthermore, the CNTs developed in our research group proved to be more attractive towards TOC abatement compared to the commercial sample.

It should be noted that this organic concentration does not represent only the quinoline compounds. It takes into account all the oxidized products or reaction intermediates after the oxidation reaction. Therefore, although quinoline could not be detected after 24 h of reaction by HPLC, there are still different organic compounds in the medium, as observed by TOC.

A similar result was shown in another study [81] that tested carbon materials as catalysts, and presented the TOC values after the CWPO reaction with a different contaminant. The values obtained varied from 42 to 100% of TOC removal in catalytic runs.

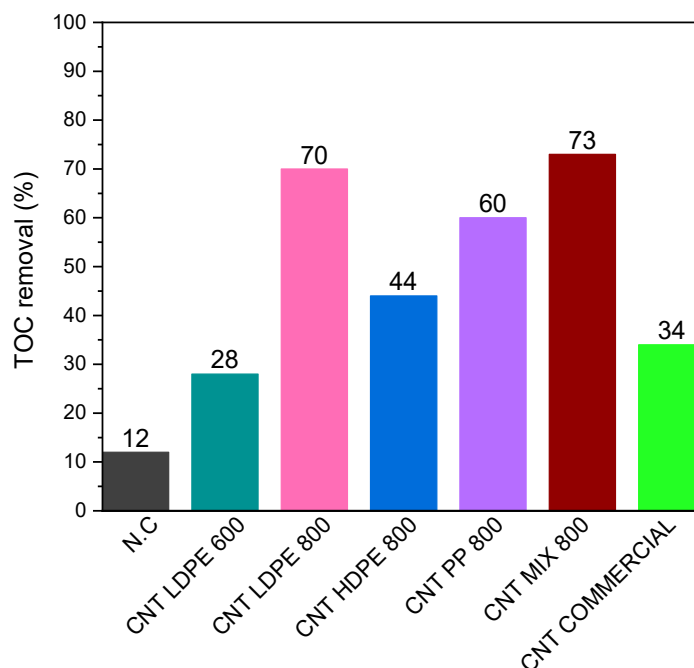


Figure 29. Percentages of TOC removal from oxidation in an aqueous system (80 °C, pH<sub>0</sub> 3, C<sub>QN</sub> = 100 mg/L in water, C<sub>CNT</sub> = 2.5 g/L, C<sub>H<sub>2</sub>O<sub>2</sub></sub> = 6.2 g/L).

#### 4.4.4 ANALYSIS OF AROMATICS IN CWPO

The percentage of aromatic removal in each CWPO run are presented in Figure 30 and considered the N.C run as calculation basis. This analysis is an approximation of aromatic amount and is not a standardized measure. Since lower amount of aromatic compounds in the medium is better, because of the possible toxicity of those unknown aromatic compounds, all the CNTs presented better results than the N.C run. The CNT that showed a better performance in this analysis was the CNT PP 800, followed by CNT COMMERCIAL, CNT MIX 800 and CNT LDPE 800 with close results, and finally CNT LDPE 600 and CNT HDPE 800.

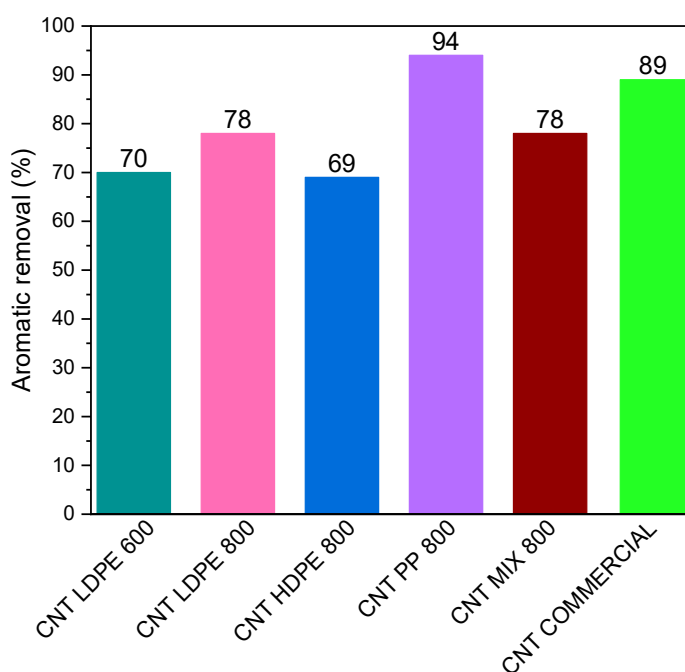


Figure 30. Aromatic removal after 24 h of run (80 °C, pH<sub>0</sub> 3, C<sub>QN</sub> = 100 mg/L in water, C<sub>CNT</sub> = 2.5 g/L, C<sub>H<sub>2</sub>O<sub>2</sub></sub> = 6.2 g/L).

#### 4.4.5 ANALYSIS OF pH IN CWPO

At the end of the CWPO runs, pH was measured, the obtained results being presented in Figure 31. The expected behaviour of pH was to decrease with the oxidation process because of the possible production of carboxylic acids upon mineralization of quinoline. But this generation of acidic compounds depends a lot on the reaction mechanism, which is affected by each catalyst activity.

The final results were close to the initial pH, except in the run carried out with CNT LDPE 600, with a final pH of 3.46, presenting the possibility of different products.

In the run with the CNT COMMERCIAL a slightly higher pH than the initial was obtained, while all the other CNTs resulted in slightly lower pHs than the initial.

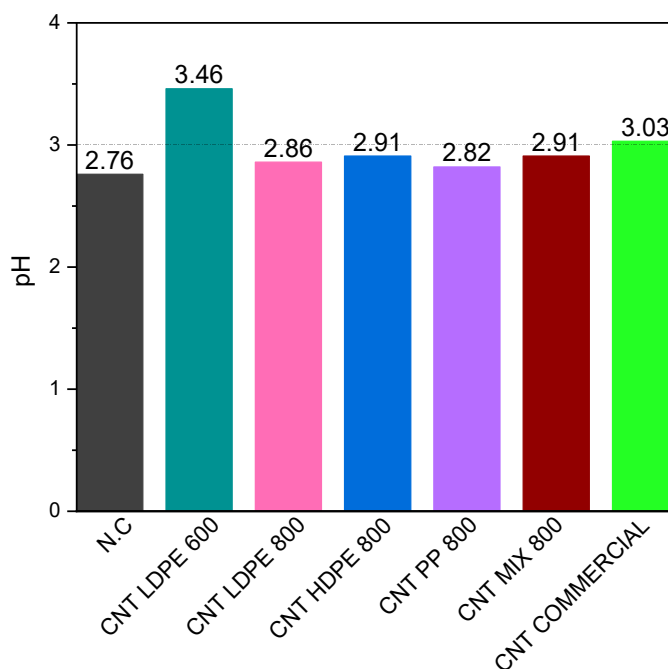


Figure 31. Analysis of pH after 24 h of CWPO run (80 °C, pH<sub>0</sub> 3, C<sub>QN</sub> = 100 mg/L in water, C<sub>CNT</sub> = 2.5 g/L, C<sub>H<sub>2</sub>O<sub>2</sub></sub> = 6.2 g/L).

#### 4.5 BIPHASIC OXIDATION

In the same way as done for the CWPO runs, the biphasic oxidation runs were also accomplished, the difference now is that both phases are considered and analysed, and quinoline was used with a concentration of 1000 mg/L in isooctane.

The runs followed the same identification as used in the CWPO run, with the first run being the non-catalytic and the next identified by the CNT's nomenclatures: CNT LDPE 600, CNT LDPE 800, CNT HDPE 800, CNT PP 800, CNT MIX 800 and CNT COMMERCIAL.

Samples of both phases were collected at different run times for hydrogen peroxide concentration and quinoline concentration analysis, and for the analysis of TOC, aromatics and pH, sample analysis was only done after 24 h run.

##### 4.5.1 CONCENTRATION OF HYDROGEN PEROXIDE IN AQUEOUS PHASE

The decomposition of H<sub>2</sub>O<sub>2</sub> in the biphasic oxidation runs carried out with the CNTs and in the non-catalytic run is presented in Figure 32. The non-catalytic run resulted

in a conversion of 47% of the initial  $\text{H}_2\text{O}_2$ . At the same time the in the runs carried out with CNTs, almost all the hydrogen peroxide was decomposed, except in the run conducted with CNT COMMERCIAL, which resulted at the end in 10% of  $\text{H}_2\text{O}_2$  remaining in the reaction medium.

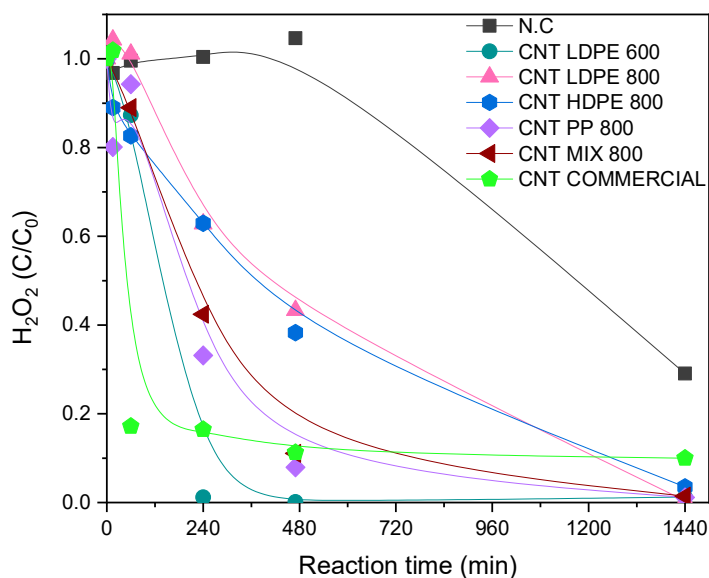


Figure 32. Concentration of hydrogen peroxide in the biphasic oxidation runs (80 °C,  $\text{pH}_0$  3 in aqueous phase,  $C_{\text{QN}} = 1000$  mg/L in isoctane,  $C_{\text{CNT}} = 2.5$  g/L,  $C_{\text{H}_2\text{O}_2} = 247$  g/L). The lines are only intended to guide the eyes.

Although in the presence of CNT COMMERCIAL, the hydrogen peroxide was not completely decomposed, it was also the CNT that resulted in the fastest decomposition, achieving a decomposition of 80% of  $\text{H}_2\text{O}_2$  in 1 h of reaction. CNT LDPE 600 also resulted in a fast decomposition of the oxidant, being able to consume it in 2 h of reaction. CNT PP 800 and CNT MIX 800 had close results during the experiments. In both cases, approximately 90% of hydrogen peroxide had already been consumed at 8 h of reaction, and complete consumption was only achieved at 24 h. CNT LDPE 800 and the CNT HDPE 800 resulted in the slowest consumption of hydrogen peroxide, with very close results during the runs. At 8 h of reaction, around 40% of the initial oxidant was still present in the reaction medium. Complete decomposition was only achieved at 24 h of reaction.

#### 4.5.2 CONCENTRATION OF QUINOLINE IN OILY PHASE

The removal of quinoline from isooctane during the biphasic oxidation was monitored by UV/VIS analysis in the oily phase. The results are displayed in Figure 33.

Figure 33 shows that the non-catalytic run led to obtaining a low removal of quinoline from the oily phase, ending up the run with 78.8% of quinoline still in the isooctane phase. In contrast, all the catalytic runs allowed to completely remove quinoline from the oily phase before 8 h of experiment. In most cases, after 4 h, quinoline was already completely removed. Complete quinoline removal was obtained at 4, 8, 4, 4, 4 and 4 h in the presence of CNT LDPE 600, CNT LDPE 800, CNT HDPE 800, CNT PP 800, CNT MIX 800 and CNT COMMERCIAL, respectively.

Furthermore, the catalytic runs are favored also by the balance between the phases: as quinoline is degraded in the aqueous phase, more quinoline is extracted from the oily phase. Similar conclusions were observed in a study about extractive and catalytic oxidative desulfurization (ECODS), in which the compounds are extracted from the oily phase to the polar extraction solvent phase, where they are oxidized, allowing the transfer of more portions of compounds from the model diesel phase [82].

All CNTs proved to be efficient in the process. The best results were obtained in the presence of CNT MIX 800, due to the faster quinoline removal from the organic phase. It can be highlighted that even though CNT COMMERCIAL resulted in the fastest hydrogen peroxide decomposition, it did not result in a faster removal of quinoline. In fact, with the exception of CNT LDPE 800, all remaining CNTs resulted in better results compared to the commercial sample.

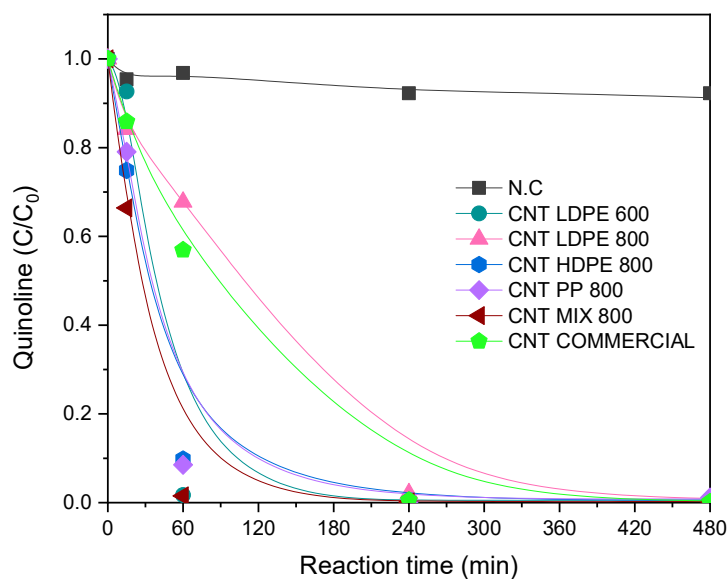


Figure 33. Concentration of quinoline in the oily phase in biphasic oxidation runs (80 °C, pH<sub>0</sub> 3 in aqueous phase,  $C_{\text{QN}} = 1000$  mg/L in isoctane,  $C_{\text{CNT}} = 2.5$  g/L,  $C_{\text{H}_2\text{O}_2} = 247$  g/L). The lines are only intended to guide the eyes.

Total removal of quinoline from the oily phase was also observed in other studies [11, 54, 55]. In those studies, all the catalytic runs were conducted in emulsified systems and with lower quinoline concentrations, such as 50 and 500 ppm in [54] and [55], respectively (in [11], quinoline concentration was not mentioned). Figure 34 shows each biphasic system after the oxidation reaction with the synthesized CNTs. There is a visible difference between the color of those systems, which could indicate the formation of different reaction intermediates (not detected).



Figure 34. Biphasic system after 24 h of oxidation reaction.

#### 4.5.3 QUINOLINE CONCENTRATION IN AQUEOUS PHASE

Figure 35 shows quinoline in the aqueous phase during the 24 h of biphasic oxidation with the different carbon materials and the non-catalytic run. As it is possible to see, the number of mol of quinoline increases with reaction time in the non-catalytic run. This increase may be ascribed to mass transfer between the organic and aqueous phase.

The accumulation of quinoline in the aqueous phase is not observed in the reaction runs conducted in the presence of the CNTs. The amount of quinoline in the aqueous phase reaches a peak in the beginning of the reaction (1 h) and then it decreases due to oxidation. This behaviour is in agreement with what was observed in the oily phase: in catalytic runs, the concentration of quinoline in the oily phase also rapidly decreased in the first 4 h of reaction.

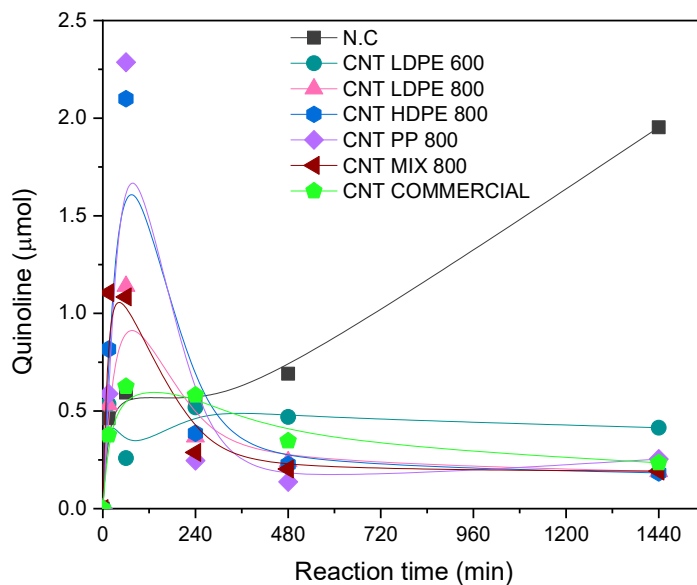


Figure 35. Quinoline quantity by UV-VIS in aqueous phase in biphasic oxidation runs (80 °C, pH<sub>0</sub> 3 in aqueous phase,  $C_{\text{QN}} = 1000$  mg/L in isooctane,  $C_{\text{CNT}} = 2.5$  g/L,  $C_{\text{H}_2\text{O}_2} = 247$  g/L). The lines are only intended to guide the eyes.

In the presence of CNT LDPE 600, CNT LDPE 800, CNT HDPE 800, CNT PP 800, CNT MIX 800 and CNT COMMERCIAL, quinoline degradation achieved conversions of 92, 96, 97, 95, 96 and 96%, respectively, in 24 h of reaction. For comparison purposes, in the same reaction time, the non-catalytic run resulted in only 63% of quinoline degradation.

Thus, all of CNTs used in the process were efficient in the oxidation of quinoline. Furthermore, the CNTs prepared by our research group displayed an equivalent behavior to the commercial sample.

In addition, the final samples from the aqueous medium were analyzed by UV/VIS to observe their spectrums. The results are depicted in Figure 36. Among the CNTs prepared in our research group, no relevant differences can be observed. However, in the presence of CNT COMMERCIAL, it is possible to observe compounds with higher absorption between 200 and 300 nm, mainly.

Nevertheless, all spectrum differs from the spectrum displayed in Figure 17a, which is related to pure quinoline spectrum. This difference between spectra obtained by the end of the reaction and the spectrum of pure quinoline can be ascribed to the formation of oxidized compounds not detected by HPLC.

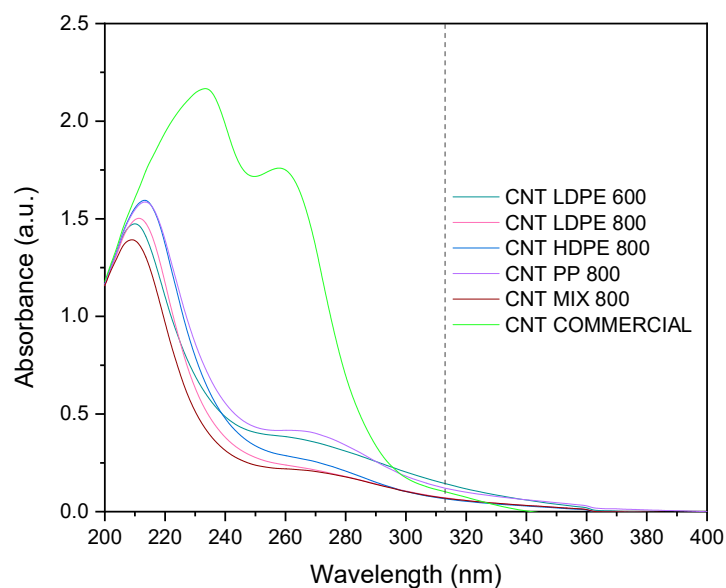


Figure 36. Final spectra of aqueous phase after the biphasic oxidation.

#### 4.5.4 TOTAL ORGANIC CARBON IN AQUEOUS PHASE

TOC analysis from the aqueous phase of the biphasic oxidations is presented in Figure 37.

As opposed to what was observed in the CWPO runs, the non-catalytic run resulted in one of the lowest values of TOC (1173 mg/L). The presence of a catalyst in the system results in a better interaction between the phases. Thus, the presence of catalyst makes the transport of the pollutant between the two phases easier. In the case of the non-catalytic run, the transport of quinoline from one phase into the other is hindered. The result is that the total organic carbon in the aqueous phase becomes lower than in the remaining catalytic processes.

For the catalytic runs, higher values of TOC were obtained. The TOC value is an accumulation of the oxidized compounds and quinoline. With the exception of the reaction carried out in the presence of CNT LDPE 600, all CNTs resulted in higher values for TOC than the non-catalytic run.

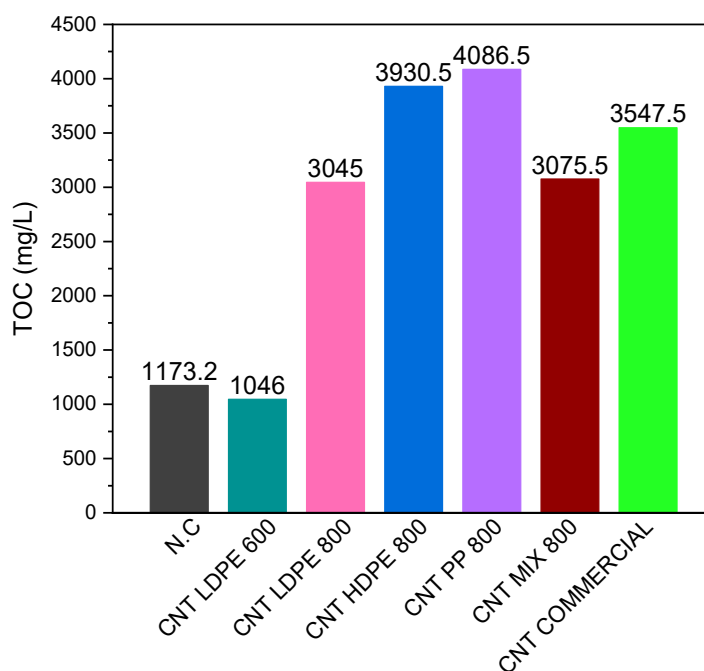


Figure 37. TOC results from aqueous phase after 24 h of biphasic oxidation runs (80 °C, pH<sub>0</sub> 3 in aqueous phase, C<sub>QN</sub> = 1000 mg/L in isooctane, C<sub>CNT</sub> = 2.5 g/L, C<sub>H<sub>2</sub>O<sub>2</sub></sub> = 247 g/L).

#### 4.5.5 AROMATIC ANALYSIS IN OILY PHASE

The estimated aromatic removal in the oily phase after 24 h is displayed in Figure 38.

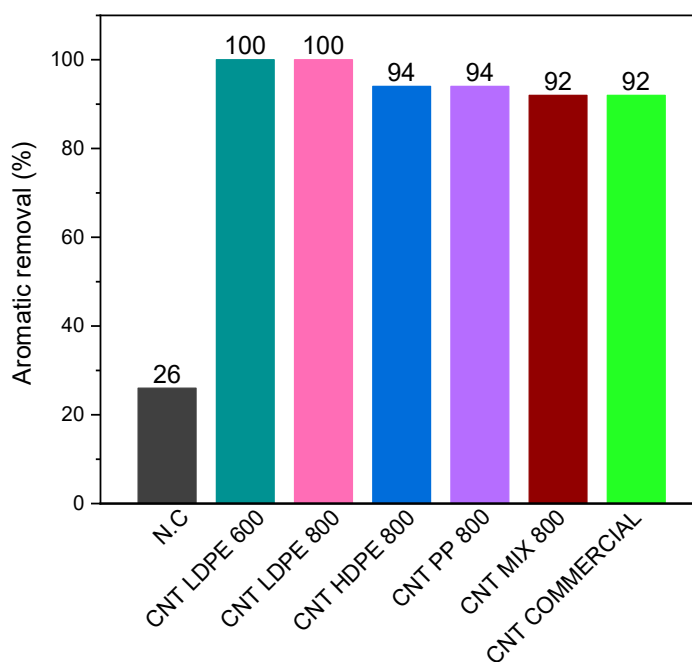


Figure 38. Aromatic removal in oily phase after 24 h of biphasic oxidation runs (80 °C, pH<sub>0</sub> 3 in aqueous phase, C<sub>QN</sub> = 1000 mg/L in isooctane, C<sub>CNT</sub> = 2.5 g/L, C<sub>H<sub>2</sub>O<sub>2</sub></sub> = 247 g/L).

All the CNTs applied were efficient in reducing the aromatic concentration compared to the non-catalytic run. The best results were obtained in the presence of CNT LDPE 600 and CNT LDPE 800, with complete removal of aromatic content.

#### 4.5.6 AROMATIC ANALYSIS IN AQUEOUS PHASE

The estimated aromatic removal in the aqueous phase is shown in Figure 39 and considered the N.C run as calculation basis.

The CNTs prepared in our research group were able to remove more aromatic content compared to the CNT COMMERCIAL, as it resulted in the lowest removal among the catalytical runs (48%). The same can be concluded by observing Figure 36, as the absorbance in the region 200 - 300 nm is much higher for reactions conducted with the commercial sample of CNT.

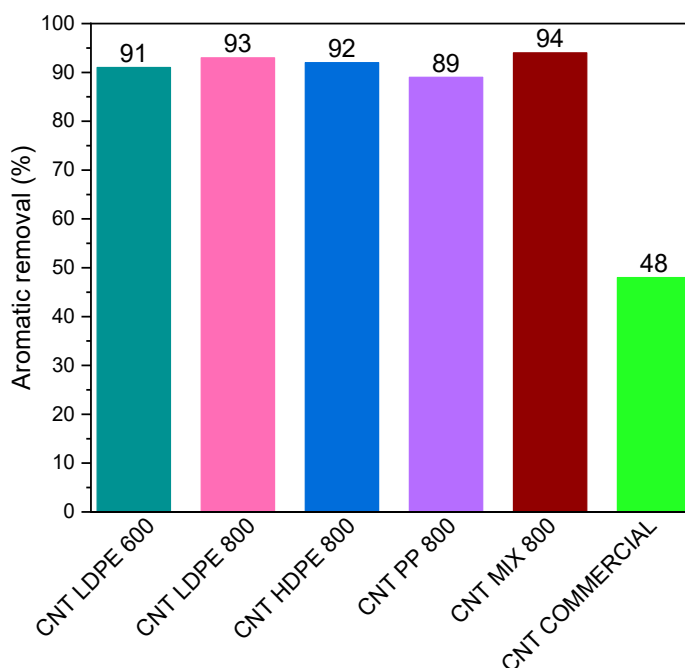


Figure 39. Aromatic removal in aqueous phase after 24 h of biphasic oxidation runs (80 °C, pH<sub>0</sub> 3 in aqueous phase, C<sub>QN</sub> = 1000 mg/L in isooctane, C<sub>CNT</sub> = 2.5 g/L, C<sub>H<sub>2</sub>O<sub>2</sub></sub> = 247 g/L).

#### 4.5.7 pH ANALYSIS IN AQUEOUS PHASE

The behavior of pH measurements at the end of the biphasic oxidations was very different from the behaviour after CWPO runs. In all biphasic oxidation runs, the pH significantly increased, as shown in Figure 40.

The pH increase can be attributed to the presence of oxidized intermediates compounds. Thus, it is expected that there is little presence of organic acids from the quinoline degradation, as opposed to the CWPO runs.

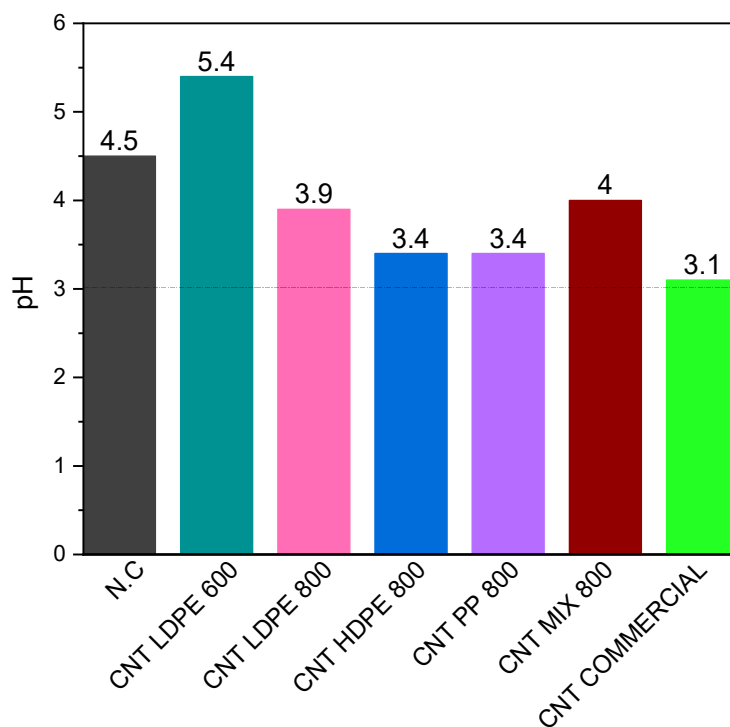


Figure 40. Analysis of pH after 24 h of biphasic oxidation runs (80 °C, pH<sub>0</sub> 3 in aqueous phase, C<sub>QN</sub> = 1000 mg/L in isooctane, C<sub>CNT</sub> = 2.5 g/L, C<sub>H<sub>2</sub>O<sub>2</sub></sub> = 247 g/L).

## 5 CONCLUSION AND FUTURE WORK

### 5.1 CONCLUSION

As a general conclusion to this present work, all the carbon nanomaterials synthesized by previous work in this research group accomplished the main goal of removing the contaminant quinoline from an organic phase (isooctane) by selective oxidation using hydrogen peroxide as oxidant in a biphasic system. In addition, all the five materials, CNT LDPE 600, CNT LDPE 800, CNT HDPE 800, CNT PP 800, and CNT MIX 800, resulted in an efficiency close, or even better to the CNT COMMERCIAL, resulting in a faster removal of the contaminant from the oily phase.

It is also possible to conclude that the CNTs act mostly as catalysts in the CWPO runs, due to the low contribution of adsorption. They were able to promote a faster degradation of H<sub>2</sub>O<sub>2</sub> and quinoline compared to the non-catalytic run. They were also able to increase the interaction of oily and aqueous phases in reactions carried out under biphasic systems, easing the mass transference between the phases, and increasing the contact between the contaminant and the oxidant in the biphasic system. This resulted in a fast removal of quinoline from the oily phase. Depending in which material was used, complete removal of quinoline was observed in less than 4 h.

The TOC and aromatics analysis for most of the catalytic runs with the CNTs synthesized in the research group, for both the CWPO runs and the biphasic oxidation, presented better results than the non-catalytic run. Thus, the catalytic systems are superior to non-catalysed processes. Furthermore, the CNTs synthesized in the research group are comparable with the commercial CNT, since close results were obtained.

Finally, the organic phase did not suffer significative oxidation in the process conditions, confirming that the selective oxidation of only the contaminant quinoline was achieved in the biphasic runs.

### 5.2 FUTURE WORK

The carbon nanotubes were synthesized from pure polymers and applied to this work. Future research could apply carbon nanotubes synthesized by real waste plastics. The oxidation process could use more than one contaminant coming from fossil fuels in the system and identify the possible reaction intermediates. The proportion between the oily and aqueous phases could be also explored. Other alternative would be to evaluate

the interferences in the process and the quantity of hydrogen peroxide used for the biphasic oxidation, as the removal of quinoline was fast in the proposed process. Lastly, the organic phase could also be exchanged by real fossil fuel to evaluate the efficiency of carbon nanomaterials in the system.

## REFERENCES

- [1] O. T. Ore and F. M. Adebisi, "A review on current trends and prospects in the pyrolysis of heavy oils," *J. Pet. Explor. Prod.*, vol. 11, no. 3, pp. 1521–1530, 2021, doi: 10.1007/s13202-021-01099-0.
- [2] "International Energy Agency," *Oil*, 2021. <https://www.iea.org/fuels-and-technologies/oil> (accessed Aug. 22, 2021).
- [3] P. Ray, "Renewable energy and sustainability," *Clean Technol. Environ. Policy*, vol. 21, no. 8, pp. 1517–1533, 2019, doi: 10.1007/s10098-019-01739-4.
- [4] M. Stylianou, I. Vyrides, and A. Agapiou, "Oil biodesulfurization: A review of applied analytical techniques," *J. Chromatogr. B Anal. Technol. Biomed. Life Sci.*, vol. 1171, no. November 2020, p. 122602, 2021, doi: 10.1016/j.jchromb.2021.122602.
- [5] U. Asghar *et al.*, "Review on the progress in emission control technologies for the abatement of CO<sub>2</sub>, SO<sub>x</sub> and NO<sub>x</sub> from fuel combustion," *J. Environ. Chem. Eng.*, vol. 9, no. 5, p. 106064, 2021, doi: 10.1016/j.jece.2021.106064.
- [6] A. Demirbas and H. S. Bamufleh, "Optimization of crude oil refining products to valuable fuel blends," *Pet. Sci. Technol.*, vol. 35, no. 4, pp. 406–412, 2017, doi: 10.1080/10916466.2016.1261162.
- [7] G. W. Huber and A. Corma, "Synergies between bio- and oil refineries for the production of fuels from biomass," *Angew. Chemie - Int. Ed.*, vol. 46, no. 38, pp. 7184–7201, 2007, doi: 10.1002/anie.200604504.
- [8] S. Badoga, P. Misra, G. Kamath, Y. Zheng, and A. K. Dalai, "Hydrotreatment followed by oxidative desulfurization and denitrogenation to attain low sulphur and nitrogen bitumen derived gas oils," *Catalysts*, vol. 8, no. 12, pp. 1–19, 2018, doi: 10.3390/catal8120645.
- [9] A. S. Ogunlaja, M. S. Abdul-quadir, P. E. Kleyi, E. E. Ferg, P. Watts, and Z. R. Tshentu, "Towards oxidative denitrogenation of fuel oils: Vanadium oxide-catalysed oxidation of quinoline and adsorptive removal of quinoline-N-oxide using 2,6-pyridine-polybenzimidazole nanofibers," *Arab. J. Chem.*, vol. 12, no. 2, pp. 198–214, 2019, doi: 10.1016/j.arabjc.2017.05.010.
- [10] J. Piera and J. Bäckvall, "Catalytic Oxidation of Organic Substrates by Molecular Oxygen and Hydrogen Peroxide by Multistep Electron Transfer — A Biomimetic Approach \*\* Angewandte," pp. 3506–3523, 2008, doi: 10.1002/anie.200700604.
- [11] I. F. Teixeira, A. A. D. S. Oliveira, T. Christofani, and F. C. C. Moura, "Biphasic oxidation promoted by magnetic amphiphilic nanocomposites undergoing a reversible emulsion process," *J. Mater. Chem. A*, vol. 1, no. 35, pp. 10203–10208, 2013, doi: 10.1039/c3ta11535f.
- [12] B. Wang, Z. Song, and L. Sun, "A review: Comparison of multi-air-pollutant removal by advanced oxidation processes – Industrial implementation for catalytic oxidation processes," *Chem. Eng. J.*, vol. 409, no. December 2020, p. 128136, 2021, doi: 10.1016/j.cej.2020.128136.
- [13] M. E. Khan, "State-of-the-art developments in carbon-based metal nanocomposites as a catalyst: photocatalysis," *Nanoscale Adv.*, vol. 3, no. 7, pp. 1887–1900, 2021, doi: 10.1039/d1na00041a.
- [14] M. Ilyas, W. Ahmad, H. Khan, S. Yousaf, K. Khan, and S. Nazir, "Plastic waste as a significant threat to environment - A systematic literature review," *Rev. Environ. Health*, vol. 33, no. 4, pp. 383–406, 2018, doi: 10.1515/revh-2017-0035.
- [15] PlasticEurope-Association of Plastics Manufacturers, "Plastics – the Facts 2020," *PlasticEurope*, pp. 1–64, 2020, [Online]. Available: <https://www.plasticseurope.org/en/resources/publications/4312-plastics-facts-2020>.
- [16] A. Rajendran, T. Y. Cui, H. X. Fan, Z. F. Yang, J. Feng, and W. Y. Li, "A comprehensive review on oxidative desulfurization catalysts targeting clean energy and environment," *J. Mater. Chem. A*, vol. 8, no. 5, pp. 2246–2285, 2020, doi: 10.1039/c9ta12555h.

- [17] S. Sukanuma and N. Katada, "Innovation of catalytic technology for upgrading of crude oil in petroleum refinery," *Fuel Process. Technol.*, vol. 208, no. July, p. 106518, 2020, doi: 10.1016/j.fuproc.2020.106518.
- [18] V. G. Yadav, G. D. Yadav, and S. C. Patankar, "The production of fuels and chemicals in the new world: critical analysis of the choice between crude oil and biomass vis-à-vis sustainability and the environment," *Clean Technol. Environ. Policy*, vol. 22, no. 9, pp. 1757–1774, 2020, doi: 10.1007/s10098-020-01945-5.
- [19] B. Bertleff *et al.*, "Extractive Catalytic Oxidative Denitrogenation of Fuels and Their Promoting Effect for Desulfurization Catalyzed by Vanadium Substituted Heteropolyacids and Molecular Oxygen," *Energy and Fuels*, vol. 34, no. 7, pp. 8099–8109, 2020, doi: 10.1021/acs.energyfuels.0c00864.
- [20] F. Rezaei, A. A. Rownaghi, S. Monjezi, R. P. Lively, and C. W. Jones, "SO<sub>x</sub>/NO<sub>x</sub> Removal from Flue Gas Streams by Solid Adsorbents: A Review of Current Challenges and Future Directions," *Energy and Fuels*, vol. 29, no. 9, pp. 5467–5486, 2015, doi: 10.1021/acs.energyfuels.5b01286.
- [21] B. Waluyo, I. N. G. Wardana, L. Yuliati, and M. N. Sasongko, "The role of molecule cluster on the azeotrope and boiling points of isooctane-ethanol blend," *Fuel*, vol. 215, no. October 2017, pp. 178–186, 2018, doi: 10.1016/j.fuel.2017.10.103.
- [22] S. Snitsiriwat and J. W. Bozzelli, "Thermochemical properties for isooctane and carbon radicals: Computational study," *J. Phys. Chem. A*, vol. 117, no. 2, pp. 421–429, 2013, doi: 10.1021/jp3041154.
- [23] D. J. Miller and S. B. Hawthorne, "Solubility of liquid organic flavor and fragrance compounds in subcritical (hot/liquid) water from 298 K to 473 K," *J. Chem. Eng. Data*, vol. 45, no. 2, pp. 315–318, 2000, doi: 10.1021/je990278a.
- [24] A. S. Ogunlaja and O. S. Alade, "Catalysed oxidation of quinoline in model fuel and the selective extraction of quinoline-N-oxide with imidazoline-based ionic liquids," *Egypt. J. Pet.*, vol. 27, no. 2, pp. 159–168, 2018, doi: 10.1016/j.ejpe.2017.02.004.
- [25] G. H. C. Prado, Y. Rao, and A. De Klerk, "Nitrogen removal from oil: A review," *Energy and Fuels*, vol. 31, no. 1, pp. 14–36, 2017, doi: 10.1021/acs.energyfuels.6b02779.
- [26] M. Ja'fari, S. L. Ebrahimi, and M. R. Khosravi-Nikou, "Ultrasound-assisted oxidative desulfurization and denitrogenation of liquid hydrocarbon fuels: A critical review," *Ultrason. Sonochem.*, vol. 40, no. September 2017, pp. 955–968, 2018, doi: 10.1016/j.ultsonch.2017.09.002.
- [27] J. C. Thermodynamics *et al.*, "Thermal behaviour of nitrogen oxides relevant to oxidative denitrogenation," *J. Chem. Thermodyn.*, vol. 136, pp. 28–43, 2019, doi: 10.1016/j.jct.2019.04.014.
- [28] X. Zhang, H. Song, C. Sun, C. Chen, F. Han, and X. Li, "Photocatalytic oxidative desulfurization and denitrogenation of fuels over sodium doped graphitic carbon nitride nanosheets under visible light irradiation," *Mater. Chem. Phys.*, vol. 226, no. September 2018, pp. 34–43, 2019, doi: 10.1016/j.matchemphys.2019.01.011.
- [29] J. Lewis and K. P. Wainwright, "Chemistry of polydentate ligands. Part 4. The oxidative denitrogenation of dichloro-6,6'-dihydrazino-2,2'-bipyridyliron(II)," *Inorganica Chim.*, vol. 34, pp. 57–60, 1979.
- [30] F. Mirante, R. F. Mendes, F. A. Almeida Paz, and S. S. Balula, "High catalytic efficiency of a layered coordination polymer to remove simultaneous sulfur and nitrogen compounds from fuels," *Catalysts*, vol. 10, no. 7, pp. 1–15, 2020, doi: 10.3390/catal10070731.
- [31] S. H. Ammar, Y. S. Kareem, and M. S. Mohammed, "Catalytic-oxidative/adsorptive denitrogenation of model hydrocarbon fuels under ultrasonic field using magnetic reduced graphene oxide-based phosphomolybdic acid (PMo-Fe<sub>3</sub>O<sub>4</sub>/rGO)," *Ultrason. Sonochem.*, vol. 64, no. March, p. 105050, 2020, doi: 10.1016/j.ultsonch.2020.105050.
- [32] B. N. Bhadra and S. H. Jung, "Oxidative desulfurization and denitrogenation of fuels using metal-organic framework-based/-derived catalysts," *Appl. Catal. B Environ.*, vol. 259, no. July, p. 118021, 2019, doi: 10.1016/j.apcatb.2019.118021.

- [33] B. N. Bhadra, Y. S. Baek, S. Kim, C. H. Choi, and S. H. Jung, "Oxidative denitrogenation of liquid fuel over W2N@carbon catalyst derived from a phosphotungstic acid encapsulated metal-azolate framework," *Appl. Catal. B Environ.*, vol. 285, no. October 2020, 2021, doi: 10.1016/j.apcatb.2020.119842.
- [34] F. Banisharif, M. R. Dehghani, M. C. Capel-Sanchez, and J. M. Campos-Martin, "Highly catalytic oxidative desulfurization and denitrogenation of diesel using anchored-silica-gel vanadium-substituted Dawson-type polyoxometalate," *Catal. Today*, vol. 333, no. July 2018, pp. 219–225, 2019, doi: 10.1016/j.cattod.2018.07.009.
- [35] B. N. Bhadra *et al.*, "Oxidative denitrogenation with TiO<sub>2</sub>@porous carbon catalyst for purification of fuel: Chemical aspects," *Appl. Catal. B Environ.*, vol. 240, no. September 2018, pp. 215–224, 2019, doi: 10.1016/j.apcatb.2018.09.004.
- [36] A. R. Martins, A. B. Salviano, A. A. S. Oliveira, R. V. Mambrini, and F. C. C. Moura, "Synthesis and characterization of catalysts based on mesoporous silica partially hydrophobized for technological applications," *Environ. Sci. Pollut. Res.*, vol. 24, no. 7, pp. 5991–6001, 2017, doi: 10.1007/s11356-016-6692-3.
- [37] A. Belinda, "DEGRADATION OF QUINOLINE BY WET OXIDATION— KINETIC ASPECTS AND REACTION MECHANISMS," *Water Reserach*, vol. 32, no. 1, pp. 136–146, 1998.
- [38] N. J. Pachupate and P. D. Vaidya, "Catalytic wet oxidation of quinoline over Ru/C catalyst," *J. Environ. Chem. Eng.*, vol. 6, no. 1, pp. 883–889, 2018, doi: 10.1016/j.jece.2017.12.014.
- [39] H. Zhu, W. Ma, H. Han, Y. Han, and W. Ma, "Catalytic ozonation of quinoline using nano-MgO: Efficacy, pathways, mechanisms and its application to real biologically pretreated coal gasification wastewater," *Chem. Eng. J.*, vol. 327, pp. 91–99, 2017, doi: 10.1016/j.cej.2017.06.025.
- [40] M. T. Carvajal and S. Yalkowsky, "Effect of pH and Ionic Strength on the Solubility of Quinoline: Back-to-Basics," *AAPS PharmSciTech*, vol. 20, no. 3, pp. 1–8, 2019, doi: 10.1208/s12249-019-1336-9.
- [41] S. L. Guseinov, S. G. Fedorov, V. A. Kosykh, and P. A. Storozhenko, "Hydrogen Peroxide Decomposition Catalysts Used in Rocket Engines," *Russ. J. Appl. Chem.*, vol. 93, no. 4, pp. 467–487, 2020, doi: 10.1134/S1070427220040011.
- [42] S. Ranganathan and V. Sieber, "Recent advances in the direct synthesis of hydrogen peroxide using chemical catalysis—a review," *Catalysts*, vol. 8, no. 9, 2018, doi: 10.3390/catal8090379.
- [43] M. Pera-Titus, L. Leclercq, J. M. Clacens, F. De Campo, and V. Nardello-Rataj, "Pickering interfacial catalysis for biphasic systems: From emulsion design to green reactions," *Angew. Chemie - Int. Ed.*, vol. 54, no. 7, pp. 2006–2021, 2015, doi: 10.1002/anie.201402069.
- [44] J. L. Diaz de Tuesta, G. F. Pantuzza, A. M. T. Silva, P. Praça, J. L. Faria, and H. T. Gomes, "Catalysts prepared with matured compost derived from mechanical-biological treatment plants for the wet peroxide oxidation of pollutants with different lipophilicity," *Catalysts*, vol. 10, no. 11, pp. 1–14, 2020, doi: 10.3390/catal10111243.
- [45] J. J. R. Márquez, I. Levchuk, and M. Sillanpää, "Application of catalytic wet peroxide oxidation for industrial and urban wastewater treatment: A review," *Catalysts*, vol. 8, no. 12, 2018, doi: 10.3390/catal8120673.
- [46] J. He, X. Yang, B. Men, and D. Wang, "Interfacial mechanisms of heterogeneous Fenton reactions catalyzed by iron-based materials: A review," *J. Environ. Sci. (China)*, vol. 39, pp. 97–109, 2016, doi: 10.1016/j.jes.2015.12.003.
- [47] C. S. D. Rodrigues, R. M. Silva, S. A. C. Carabineiro, F. J. Maldonado-Hódar, and L. M. Madeira, "Wastewater treatment by catalytic wet peroxidation using nano gold-based catalysts: A review," *Catalysts*, vol. 9, no. 5, 2019, doi: 10.3390/catal9050478.
- [48] B. Bethi, S. H. Sonawane, B. A. Bhanvase, and S. P. Gumfekar, "Nanomaterials-based advanced oxidation processes for wastewater treatment: A review," *Chem. Eng. Process. Process Intensif.*, vol. 109, pp. 178–189, 2016, doi: 10.1016/j.cep.2016.08.016.
- [49] M. Coha, G. Farinelli, A. Tiraferri, M. Minella, and D. Vione, "Advanced oxidation processes in

- the removal of organic substances from produced water: Potential, configurations, and research needs,” *Chem. Eng. J.*, vol. 414, no. January, p. 128668, 2021, doi: 10.1016/j.cej.2021.128668.
- [50] R. Guan, X. Yuan, Z. Wu, L. Jiang, and Y. Li, “Principle and application of hydrogen peroxide based advanced oxidation processes in activated sludge treatment : A review,” *Chem. Eng. J.*, vol. 339, no. November 2017, pp. 519–530, 2018, doi: 10.1016/j.cej.2018.01.153.
- [51] S. Subhan, Y. Muhammad, M. Sahibzada, F. Subhan, and Z. Tong, “Studies on the Selection of a Catalyst-Oxidant System for the Energy-Efficient Desulfurization and Denitrogenation of Fuel Oil at Mild Operating Conditions,” *Energy and Fuels*, vol. 33, no. 9, pp. 8423–8439, 2019, doi: 10.1021/acs.energyfuels.9b01950.
- [52] M. Vafaezadeh and W. R. Thiel, “Janus interphase catalysts for interfacial organic reactions,” *J. Mol. Liq.*, vol. 315, p. 113735, 2020, doi: 10.1016/j.molliq.2020.113735.
- [53] I. R. Guimarães, A. S. Giroto, W. F. De Souza, and M. C. Guerreiro, “Highly reactive magnetite covered with islands of carbon: Oxidation of N and S-containing compounds in a biphasic system,” *Appl. Catal. A Gen.*, vol. 450, pp. 106–113, 2013, doi: 10.1016/j.apcata.2012.10.017.
- [54] R. V. Mambrini, C. Z. Maia, J. D. Ardisson, P. P. De Souza, and F. C. C. Moura, “Fe/C and FeMo/C hybrid materials for the biphasic oxidation of fuel contaminants,” *New J. Chem.*, vol. 41, no. 1, pp. 142–150, 2016, doi: 10.1039/C6NJ02718K.
- [55] A. D. Purceno *et al.*, “Magnetic amphiphilic hybrid carbon nanotubes containing N-doped and undoped sections: Powerful tensioactive nanostructures,” *Nanoscale*, vol. 7, no. 1, pp. 294–300, 2015, doi: 10.1039/c4nr04005h.
- [56] A. A. S. Oliveira *et al.*, “N-doped carbon nanotubes grown on red mud residue: Hybrid nanocomposites for technological applications,” *Catal. Today*, vol. 344, no. April, pp. 247–258, 2020, doi: 10.1016/j.cattod.2019.04.060.
- [57] A. A. S. Oliveira, I. F. Teixeira, T. Christofani, J. C. Tristão, I. R. Guimarães, and F. C. C. Moura, “Biphasic oxidation reactions promoted by amphiphilic catalysts based on red mud residue,” *Appl. Catal. B Environ.*, vol. 144, no. 1, pp. 144–151, 2014, doi: 10.1016/j.apcatb.2013.07.015.
- [58] W. D. do Pim *et al.*, “A pH-triggered bistable copper(ii) metallacycle as a reversible emulsion switch for biphasic processes,” *Chem. Commun.*, vol. 49, no. 92, pp. 10778–10780, 2013, doi: 10.1039/c3cc46242k.
- [59] Z. Xie, Z. Liu, Y. Wang, Q. Yang, L. Xu, and W. Ding, “An overview of recent development in composite catalysts from porous materials for various reactions and processes,” *Int. J. Mol. Sci.*, vol. 11, no. 5, pp. 2152–2187, 2010, doi: 10.3390/ijms11052152.
- [60] L. C. A. de Oliveira, N. T. Costa, J. R. Pliego, A. C. Silva, P. P. de Souza, and P. S. Patrícia, “Amphiphilic niobium oxyhydroxide as a hybrid catalyst for sulfur removal from fuel in a biphasic system,” *Appl. Catal. B Environ.*, vol. 147, pp. 43–48, 2014, doi: 10.1016/j.apcatb.2013.08.003.
- [61] X. Sun, R. Wang, and D. Su, “Research progress in metal-free carbon-based catalysts,” *Cuihua Xuebao/Chinese J. Catal.*, vol. 34, no. 3, pp. 508–523, 2013, doi: 10.1016/s1872-2067(11)60515-9.
- [62] G. de Freitas Batista, F. F. Roman, J. L. D. de Tuesta, R. V. Mambrini, P. Praça, and H. T. Gomes, “Assessment of Pretreatments for Highly Concentrated Leachate Waters to Enhance the Performance of Catalytic Wet Peroxide Oxidation with Sustainable Low-Cost Catalysts,” *Catalysts*, vol. 12, no. 2, p. 238, 2022, doi: 10.3390/catal12020238.
- [63] J. L. Diaz de Tuesta, B. F. Machado, P. Serp, A. M. Adrián, J. L. Faria, and H. T. Gomes, “Janus amphiphilic carbon nanotubes as Pickering interfacial catalysts for the treatment of oily wastewater by selective oxidation with hydrogen peroxide,” *Catal. Today*, vol. 356, no. February 2019, pp. 205–215, 2020, doi: 10.1016/j.cattod.2019.07.012.
- [64] S. TANG *et al.*, “Review of New Carbon Materials as Catalyst Supports in Direct Alcohol Fuel Cells,” *Chinese J. Catal.*, vol. 31, no. 1, pp. 12–17, 2010, doi: 10.1016/s1872-2067(09)60034-6.
- [65] M. Endo, T. Hayashi, Y. A. Kim, and H. Muramatsu, “Development and application of carbon nanotubes,” *Japanese J. Appl. Physics, Part 1 Regul. Pap. Short Notes Rev. Pap.*, vol. 45, no. 6 A,

- pp. 4883–4892, 2006, doi: 10.1143/JJAP.45.4883.
- [66] R. Rocha, O. Soares, J. Figueiredo, and M. Pereira, “Tuning CNT Properties for Metal-Free Environmental Catalytic Applications,” *C*, vol. 2, no. 3, p. 17, 2016, doi: 10.3390/c2030017.
- [67] A. Bazargan and G. McKay, “A review - Synthesis of carbon nanotubes from plastic wastes,” *Chem. Eng. J.*, vol. 195–196, pp. 377–391, 2012, doi: 10.1016/j.cej.2012.03.077.
- [68] C. Zhuo and Y. A. Levendis, “Upcycling waste plastics into carbon nanomaterials: A review,” *J. Appl. Polym. Sci.*, vol. 131, no. 4, pp. 1–14, 2014, doi: 10.1002/app.39931.
- [69] D. Yao, H. Yang, Q. Hu, Y. Chen, H. Chen, and P. T. Williams, “Carbon nanotubes from post-consumer waste plastics: Investigations into catalyst metal and support material characteristics,” *Appl. Catal. B Environ.*, vol. 280, no. April 2020, p. 119413, 2021, doi: 10.1016/j.apcatb.2020.119413.
- [70] S. Ravi and S. Vadukumpully, “Sustainable carbon nanomaterials: Recent advances and its applications in energy and environmental remediation,” *J. Environ. Chem. Eng.*, vol. 4, no. 1, pp. 835–856, 2016, doi: 10.1016/j.jece.2015.11.026.
- [71] A. L. Andrady and M. A. Neal, “Applications and societal benefits of plastics,” *Philos. Trans. R. Soc. B Biol. Sci.*, vol. 364, no. 1526, pp. 1977–1984, 2009, doi: 10.1098/rstb.2008.0304.
- [72] J. Hopewell, R. Dvorak, and E. Kosior, “Plastics recycling: Challenges and opportunities,” *Philos. Trans. R. Soc. B Biol. Sci.*, vol. 364, no. 1526, pp. 2115–2126, 2009, doi: 10.1098/rstb.2008.0311.
- [73] K. R. Bukkarapu, D. S. Gangadhar, Y. Jyothi, and P. Kanasani, “Management, conversion, and utilization of waste plastic as a source of sustainable energy to run automotive: a review,” *Energy Sources, Part A Recover. Util. Environ. Eff.*, vol. 40, no. 14, pp. 1681–1692, 2018, doi: 10.1080/15567036.2018.1486898.
- [74] W. Story, “Chapter 1 INTRODUCTION,” *An Autom. Irrig. Syst. Using Arduino Microcontroller*, vol. 1908, no. January, pp. 2–6, 2011.
- [75] P. T. Handbook, “1.3 Polymerization Reactions,” pp. 20–36, 2021.
- [76] M. Chanda and S. Roy, “Trends in Polymer Applications,” *Plast. Technol. Handbook, Fourth Ed.*, pp. 7-1-1–50, 2006, doi: 10.1201/9781420006360.ch7.
- [77] C. M. Masso, H. T. Gomes, J. M. T. Pietrobelli, and J. L. D. De Tuesta, “Valorization of compost in the production of carbon-based materials for the treatment of contaminated wastewater Valorization of compost in the production of carbon-based materials for the treatment of contaminated wastewater,” *Mestr. IPB*, pp. 1–62, 2018.
- [78] A. K. Reineke, T. Göen, A. Preiss, and J. Hollender, “Quinoline and derivatives at a tar oil contaminated site: Hydroxylated products as indicator for natural attenuation?,” *Environ. Sci. Technol.*, vol. 41, no. 15, pp. 5314–5322, 2007, doi: 10.1021/es070405k.
- [79] S. H. Standal, A. M. Blokhus, J. Haavik, A. Skauge, and T. Barth, “Partition coefficients and interfacial activity for polar components in oil/water model systems,” *J. Colloid Interface Sci.*, vol. 212, no. 1, pp. 33–41, 1999, doi: 10.1006/jcis.1998.5988.
- [80] J. R. D. V. J.B. de H. Alonso, J.T. Antón, T.G. Montero, “Análisis químico de aguas residuales,” 2004.
- [81] M. Martin-Martinez *et al.*, “Carbon nanotubes as catalysts for wet peroxide oxidation: The effect of surface chemistry,” *Catal. Today*, vol. 357, no. February, pp. 332–340, 2020, doi: 10.1016/j.cattod.2019.03.014.
- [82] A. C. Gomes, D. Juli, M. Pillinger, I. S. Gonc, and S. S. Balula, “Dichloro and dimethyl dioxomolybdenum ( VI ) -bipyridine complexes as catalysts for oxidative desulfurization of dibenzothiophene derivatives under extractive conditions,” *J. Organomet. Chem.*, no. Vi, p. 122336, 2022, doi: 10.1016/j.jorganchem.2022.122336.

## **ATTACHMENTS**

As a result of the work, a paper was submitted to the IX CARBOCAT, 9<sup>th</sup> INTERNATIONAL SYMPOSIUM ON CARBON FOR CATALYST, which was approved for oral presentation and used data collected in this work. The file can be seen below.

## OXIDATIVE DENITROGENATION WITH H<sub>2</sub>O<sub>2</sub> OF A SIMULATED FUEL UNDER A BIPHASIC SYSTEM BY SUSTAINABLE CARBON NANOTUBES

Larissa de G. Piccinin<sup>1,2</sup>, Fernanda F. Roman<sup>1,3\*</sup>, Isabella V. de Freitas<sup>1,4</sup>, Jose L. Diaz de Tuesta<sup>1</sup>, Adrián M. T. Silva<sup>3</sup>, Joaquim L. Faria<sup>3</sup>, Admilson Lopes Vieira<sup>2</sup>, Giane G. Lenzi<sup>4</sup>, Helder T. Gomes<sup>1</sup>

<sup>1</sup>Centro de Investigação de Montanha (CIMO), Instituto Politécnico de Bragança, 5300-253 Bragança, Portugal

<sup>2</sup>Universidade Tecnológica Federal do Paraná, Campus Londrina, 86036-370 Londrina, Brasil

<sup>3</sup>Laboratory of Separation and Reaction Engineering – Laboratory of Catalysis and Materials (LSRE-LCM), Faculdade de Engenharia, Universidade do Porto, 4200-465 Porto, Portugal

<sup>4</sup>Universidade Tecnológica Federal do Paraná, Campus Ponta Grossa, 84017-220 Ponta Grossa, Brasil

\*roman@ipb.pt

The presence of nitrogenated compounds in liquid fuels is associated with a series of environmental and health issues [1], as upon their combustion, NO<sub>x</sub> gases are formed. Normally, those heteroatoms are removed through a process called hydrodenitrogenation (HDN), which is based on H<sub>2</sub> under high temperature and pressure. However, due to the type of nitrogenated compounds found in crude oils, which consist mostly of cyclic structures containing two double bonds between N and C, HDN fails to efficiently remove nitrogen without affecting the properties of the fuel [1]. Thus, alternatives to HDN have been sought, and a promising alternative is the removal of those nitrogenated compounds via oxidative processes [1]. In the oxidative denitrogenation (ODN), the nitrogen-based compounds are oxidized towards more polar compounds, which can be further removed by an extractant. Furthermore, another contemporary issue is the production and accumulation of residues, especially plastic solid waste (PSW). This PSW can be used as precursors for the synthesis of more sustainable carbon nanotubes (CNTs), which could be further applied as catalysts in ODN. In this work, a nitrogen-rich fuel was simulated by dissolving quinoline (QN, C<sub>2,2,4-trimethylpentane,0</sub> = 1 g L<sup>-1</sup>) in 2,2,4-trimethylpentane (*i*-octane), and ODN was carried out using H<sub>2</sub>O<sub>2</sub> as the oxidant source and CNTs derived from a mixture of polymers simulating PSW as catalysts, under a biphasic system (oxidation and extraction co-occur).

CNT was synthesized via chemical vapour deposition (CVD), considering an iron-based material supported in alumina (Fe/Al<sub>2</sub>O<sub>3</sub>) as catalyst and a mixture of polymers as carbon sources (low-density polyethylene, high-density polyethylene, and polypropylene, in a proportion of 35:25:40 (mass basis)). CVD was conducted at 800 °C under nitrogen atmosphere (40 mL min<sup>-1</sup>) for 1 h, considering 5 g of the polymer mixture and 1 g of Fe/Al<sub>2</sub>O<sub>3</sub>, leading to CNT-MIX. CNT-MIX was subjected to acid washing under reflux (50% vol. H<sub>2</sub>SO<sub>4</sub>, 140 °C, 3 h). ODN was carried out at 80 °C in a biphasic system (*i*-octane:aqueous phase) at a volume ratio of 80:20 for 1 h. The initial pH of the aqueous phase was set to 3 by means of a 1 M H<sub>2</sub>SO<sub>4</sub> solution, and the concentration of H<sub>2</sub>O<sub>2</sub> was chosen as 10 times the stoichiometric amount for complete QN degradation. CNT-MIX and a CNT commercial sample (Sigma-Aldrich) were tested as catalysts ( $C_{cat} = 2.5 \text{ g L}^{-1}$ , considering the total volume of the reaction). A non-catalytic run (N.C.) was also considered for comparison. QN was measured by UV-Vis in both oily and aqueous phase at a wavelength of 313 nm. Adsorption and extraction-only studies were also carried out under the same conditions for comparison. Oxidation of *i*-octane was assessed without the presence of QN and it was found it was negligible under the operating conditions.

The results are summarized in Fig. 1. As it can be seen, extraction-only hardly removes any QN from the oily phase. Similarly, adsorption can only account for a removal in the range of 4-10% of QN depending on the catalyst used. Adding only H<sub>2</sub>O<sub>2</sub> without catalyst (N.C.) has not impact on the removal of QN. On the other hand, ODN experiments were able to almost remove QN fully from *i*-octane (98% in 1 h of reaction) considering the sustainable CNT-MIX, reaching 99.8% of QN removal in 2 h of reaction (data not shown), which greatly surpassed the results obtained in the presence of the commercial CNT sample (only 43% removal after 1 h). Thus, these results suggest that it is a viable option to upcycle PSW into CNTs for effective removal of hazardous compounds from oily phases.

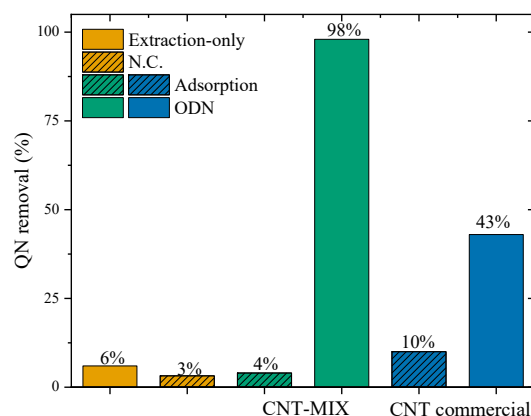


**Figure 1.** QN removal by extraction, adsorption and ODN considering CNTs as catalysts. (Conditions: **ODN:** *i*-octane:aqueous phase = 80:20,  $C_{i\text{-octane},0} = 1 \text{ g L}^{-1}$ ,  $pH_{\text{aqueous phase},0} = 3.0$ ,  $C_{H_2O_2,0} = 10 \times$  stoichiometric amount for QN degradation,  $C_{cat} = 2.5 \text{ g L}^{-1}$ ,  $T = 80 \text{ }^\circ\text{C}$ , 1 h; **Adsorption:** *i*-octane:aqueous phase = 80:20,  $C_{i\text{-octane},0} = 1 \text{ g L}^{-1}$ ,  $pH_{\text{aqueous phase},0} = 3.0$ ,  $C_{cat} = 2.5 \text{ g L}^{-1}$ ,  $T = 80 \text{ }^\circ\text{C}$ , 1 h; **Extraction:** *i*-octane:aqueous phase = 80:20,  $C_{i\text{-octane},0} = 1 \text{ g L}^{-1}$ ,  $pH_{\text{aqueous phase},0} = 3.0$ ,  $T = 80 \text{ }^\circ\text{C}$ , 1 h)

**Acknowledgements.** This work was financially supported by project "PLASTIC TO FUEL&MAT – Upcycling Waste Plastics into Fuel and Carbon Nanomaterials" (PTDC/EQU-EQU/31439/2017), Base Funding - UIDB/50020/2020 of the Associate Laboratory LSRE-LCM - funded by national funds through FCT/MCTES (PIDDAC), and CIMO (UIDB/00690/2020) through FEDER under Program PT2020. Fernanda F. Roman acknowledges the national funding by FCT, Foundation for Science and Technology, and FSE, European Social Fund, through the individual research grant SFRH/BD/143224/2019.

[1] F. F. Roman, J. L. Diaz de Tuesta, A. M. T. Silva, J. L. Faria, H. T. Gomes. *Catalysts*, 11 (2021) 1239.